[AMERICAN JOURNAL OF SCIENCE, VOL. 294, JANUARY, 1994, P. 92–135]

APATITE IN FELSIC ROCKS: A MODEL FOR THE ESTIMATION OF INITIAL HALOGEN CONCENTRATIONS IN THE BISHOP TUFF (LONG VALLEY) AND TUOLUMNE INTRUSIVE SUITE (SIERRA NEVADA BATHOLITH) MAGMAS*

PHILIP PICCOLI and PHILIP CANDELA
Laboratory for Mineral Deposits Research, Department of Geology, University of Maryland, College Park, Maryland 20742

ABSTRACT. Variations in the concentration of the halogens in apatite can be used to deduce changes in fugacity ratios during the crystallization of intrusive and extrusive felsic rocks. In addition, a model initial concentration of Cl and F in the melt and the associated magmatic volatile phase (MVP) can be calculated if the temperature of apatite crystallization in the system can be approximated. Model apatite saturation temperatures (AST) can be calculated, given appropriate apatite solubility data in silicate melts, by assuming that the initial melt composition is equal to the whole rock composition and that apatite has crystallized from the melt.

Our calculations suggest that apatite began to crystallize at 860°C in the plinian phase of the Bishop Tuff (PBT) based on published whole rock P_2O_5 data. This AST of 860°C has been used in conjunction with published apatite analyses to yield estimates of initial aqueous phase Cl (31,000-42,000 ppm) and F (38-60 ppm) concentrations. These values suggest 700-960 ppm Cl and 160-300 ppm F in the initial melt given reasonable estimates of the melt/volatile partitioning of Cl and F. These preliminary estimates of initial magmatic Cl and F compare favorably with published compositional data on melt inclusions from the Bishop Tuff.

Applying these calculations to the Tuolumne Intrusive Suite and accounting for melt composition as a function of crystallinity yield the following AST values (°C): Kuna Crest (KC) 928, Half Dome Equigranular (HDE) 901, Half Dome Porphyry (HDP) 915, Cathedral Peak (CP) 925, and Johnson Porphyry (JP) 795. These temperatures are all below the respective liquidus temperatures for reasonable water contents. The AST values are fairly constant across the suite, except for the JP. Consideration of apatite solubility data suggests that over half the apatite crystallizes within 60°C of the AST for the KC, HDE, HDP, and CP and within 30°C for the JP. The proportion of the melt that crystallizes before apatite saturation has also been estimated: KC (35 percent), HDE (9 percent), HDP (9 percent), CP (9 percent), and JP (16 percent). The ratio of the mole fraction of chlorapatite to hydroxyapatite ($X^{Ap}_{ClAp}/X^{Ap}_{HAp}$) decreases and fluorapatite to hydroxyapatite ($X^{Ap}_{FAp}/X^{Ap}_{HAp}$) increases within the host rocks from the outer to the inner units of the Tuolumne Instrusive Suite: KC (0.08, 1.7). HDE (0.06, 4.6), HDP (0.02, 2.7), CP (0.03, 5.0) and JP (0.02, 8.0). Given this information, the following concentrations (in ppm) for Cl and F, respectively, in the magmatic volatile phase have been estimated: KC (27,000; 46), HDE

*Laboratory for Mineral Deposits Research Contribution #24.

(19,000; 98), HDP (6000; 66), CP (10,000; 130), and JP (3000; 31). The initial melt is estimated to contain the following concentrations of Cl and F (in ppm), respectively: KC (400; 100-150), HDE (400; 320-430), HDP (130; 210-290), CP (210; 400-590), and JP (58; 240-290). This drop in initial Cl in the melt from the outer to the inner units of the Tuolumne Intrusive Suite corresponds well with the increase in $(^{87}Sr/^{86}Sr)_i$ and decrease in $\epsilon_{Nd}(T)$ determined by other workers. The relationship between decreasing Cl and increasing $(^{87}Sr/^{86}Sr)_i$ and decreasing $\epsilon_{Nd}(T)$ suggests that variations in initial Cl in the melt in this system may be controlled by variable amounts of a subduction related component in the magmatic source region.

SYMBOLS

X_i^ϕ	mole fraction of phase component i in phase ϕ
C_i^j	concentration of i in melt
$C_i^{l,o}$	concentration of i in initial melt
$C_i^{l,AST}$	concentration of i in the melt at the apatite saturation temperature
$D_i^{aq,l}$	partition coefficient of i between the magmatic volatile phase and melt
f_i^ϕ	fugacity of phase component i in ϕ
a_i^ϕ	activity of phase component i in ϕ
$a_i^{l,AST}$	activity of i in the melt at the apatite saturation temperature
$a_i^{l,QSAT}$	activity of i in the melt at quartz saturation
γ_i^ϕ	activity coefficient of phase component i in ϕ
m_i^j	molality of i in j
μ_i^ϕ	chemical potential of phase component i in ϕ
ΣCl^{aq}	total Cl in the magmatic volatile phase ($\Sigma Cl^{aq} = NaCl^{aq} + KCl^{aq} + 2FeCl_2^{aq}$, et cetera)
n	refractive index

INTRODUCTION

The spatial and temporal relationships between felsic igneous rocks and porphyry and skarn type deposits suggest "magmatic volatile components" (defined here as H_2O, O_2, HCl, HF, or $Cl(OH)_{-1}$, $F(OH)_{-1}$, et cetera) play an important part in ore genesis. The relationship between fugacities of magmatic volatile components and associated ore metal concentrations in deposits has been reported frequently; however, due to the inability to sample magmatic-hydrothermal ore fluids directly, we must address alternative methods to obtain estimates of halogen concentrations in the magmatic volatile phase.

Several hydrous minerals, including apatite, biotite, and hornblende, can crystallize from felsic magmas. These minerals also admit chloride and fluoride in the hydroxyl site and can be used to estimate the relative activities (or fugacities) of H_2O, HCl, and HF. More precisely, the

chemistry of hydrous minerals, together with appropriate thermodynamic data, can be used to estimate relative changes in the chemical potential of the exchange components $Cl(OH)_{-1}$ and $F(OH)_{-1}$ (which will be referred to herein as exchange potentials (Thompson, 1982)).

Various workers have examined the feasibility of using the halogen (defined here as Cl and F) concentrations in biotite as measures of exchange potentials and as indicators of the economic grade of high-temperature hydrothermal mineral deposits (Stollery, Borcsik, and Holland, 1971; Parry, 1972; Parry and Jacobs, 1975; Kesler and others, 1975; Munoz, 1990; Gunow, ms). More recently, Ague and Brimhall (1988a,b) use the fluid composition as estimated from biotites to identify the presence and extent of contamination of granitic magmas. Their approach is fruitful because biotite is common in felsic magmatic rocks and typically has a fairly large grain size which is necessary for microanalysis. The relationship Ague and Brimhall found between $\mu_{Fe(Mg)_{-1}}$ and $\mu_{F(OH)_{-1}}$ in biotite shed much light on granite genesis. Regarding chlorine, however, several workers (Volfinger and others, 1985; Munoz, 1990) have suggested that the systematics governing the Cl–OH exchange between micas and aqueous fluids are complex and do not simply reflect the $Cl(OH)_{-1}$ exchange potential in associated fluids. Further, it has been suggested by Roegge and others (1974), Parry and Jacobs (1975), and most recently by Tacker and Stormer (1989) and Munoz (1990) that apatite is not as vulnerable as micas to subsolidus chlorine-hydroxyl exchange and may not be subject to crystal-chemical effects on halogen concentration (Munoz, 1990, and personal communication).

The temperature dependence on the halogen-hydroxyl exchange between apatite and aqueous fluids has been recognized for some time, and equilibrium constants have been determined (Korzhinskiy, 1981; Tacker and Stormer, 1989; Zhu and Sverjensky, 1991). This temperature dependence has been used to estimate the compositions of fluids associated with volcanic rocks (Crisp and Spera, 1987; Piccoli and Candela, 1988; Tacker, 1988), intrusive rocks (Piccoli and Candela, 1991, 1992; Boudreau, Mathez, and McCallum, 1986; Boudreau and McCallum, 1989; Boudreau and Kruger, 1990) and metamorphic rocks (Sisson, 1987; Yardley, 1985). However, all these studies make use of estimates of fugacity ratios of hydrogen-halides and not actual concentrations of halogens in the fluid phases in question.

We present a detailed discourse on the role of mineral-melt solubility data to estimate temperature and crystallization systematics of apatite in silicic systems. This is an improvement on present methods in which estimates of fugacity ratios are calculated based on mineral-melt equilibria in that we are not assuming a temperature of crystallization as has been done in prior studies, and we use available melt/aqueous phase partitioning data to make estimates of magmatic halogen concentrations (not fugacities of hydrogen-halides).

In this paper, we present a model in which the halogen concentration in apatite can be used to estimate the initial halogen content of

metaluminous, felsic magmas. The model is designed to simulate a magma that exsolves a magmatic volatile phase due to crystallization at a constant pressure (second boiling). Some of the experimental data utilized in these calculations have rather large uncertainties; however, first order estimates of initial halogen concentrations in magmas can be made by use of this model. The calculation will be applied to one volcanic example, the Bishop Tuff of Long Valley, and one plutonic example, the Tuolumne Intrusive Suite of the Sierra Nevada batholith.

THE MODEL

The first step in this analysis is to calculate the solubility of apatite in the magma composition of interest. As a silicate melt cools it will become saturated with apatite and other crystalline phases. According to Harrison and Watson (1984), the temperature and SiO_2 concentrations in the melt are the two most important parameters needed to calculate the solubility of apatite in cooling metaluminous magmas (in peraluminous rocks aluminosity is also an important variable; for example Pichavant, Montel, and Richard, 1992). If we assume that the melt composition is determined by magma mixing, without any significant crystal settling, then the whole rock composition may represent the original melt composition. Therefore, the solubility of apatite in the magma can be calculated for magma compositions of interest, given estimates of how melt SiO_2 and P_2O_5 concentrations change as the magma crystallizes. In this way, the apatite saturation temperature (AST) and the amount of apatite crystallized for a given cooling interval (ΔT) can be calculated. Second, apatite is analyzed from a suite of rocks by electron probe microanalysis (or an alternative appropriate technique) for Cl and F, and the mole fractions of chlorapatite (ClAp), fluorapatite (FAp) and hydroxyapatite (HAp) are calculated. The third step is to calculate the composition of the magmatic volatile phase that would be in equilibrium with the apatites analyzed in the second step at the respective AST value given in step one. This is accomplished by using published thermodynamic data on the pertinent apatite and magmatic volatile components. The fourth step is to calculate the total Cl in the magmatic volatile phase from the relationship between HCl and total chloride ($\Sigma Cl^{aq} = HCl^{aq} + NaCl^{aq} + KCl^{aq} + 2FeCl_2^{aq}$, et cetera) for the given melt composition. Calculations by Zhu and Sverjensky (1991) suggest that most of the F in the magmatic volatile phase is present as HF (over 99.9 percent HF) under conditions similar to those assumed in these calculations, so a similar calculation for F does not need to be performed. The final step in the analysis is to calculate the melt chloride and fluoride concentrations, if a magmatic volatile phase is present at the AST, using magmatic volatile phase/melt partitioning data and the aqueous-halide concentration. Additionally, initial halogen concentrations in the melt can be obtained using estimates of melt crystallization preceding apatite saturation assuming incompatible behavior of the halogens.

These equations are then used to calculate the concentrations of the halogens in the melt for several magmatic systems. These calculations are currently setup to model the exsolution of a magmatic volatile phase due to second boiling at pressures between 1.6 to 2.0 kb. However, this method can be modified to simulate crystallization under other conditions with caution.

CONDITIONS AT APATITE SATURATION

Temperature

Strong temperature dependence on apatite/melt exchange equilibria has been recognized for some time, and it is therefore important to determine the temperature at which apatite crystallizes when making estimates of magmatic halogen concentrations. Apatite crystallizes over a wide temperature range. Estimates of the temperature at which apatite begins to crystallize were made previously (Clemens, Holloway, and White, 1986; Kogarko and Romanchev, 1990); however, up to this time, they have not been used in the estimation of the halogen concentrations of felsic magmas.

Estimations of apatite crystallization temperature can be obtained by comparing natural and experimental systems. Extensive experiments have been completed by Harrison and Watson (1984), Watson and Harrison (1984), Green and Watson (1982), and Watson (1979, 1980) on the solubility of apatite in melts of natural composition. Harrison and Watson found that for metaluminous melts with $C^{l,o}_{SiO_2}$ of 45 to 75 percent, $C^{l,o}_{H_2O}$ of 0 to 10 percent, and at pressures exhibited in the crust, the solubility of apatite could be expressed as a function of temperature and the instantaneous $C^{l}_{SiO_2}$ and $C^{l}_{P_2O_5}$ at which the apatite crystallizes. The effects of water concentration, pressure, and the concentration of calcium on apatite solubility were not significant *independent* controls on apatite solubility within the rather narrow confines of the basalt–dacite–rhyolite temperature-composition space and the limits of precision of their experiments. Experiments have been performed on apatite solubilities in peraluminous melts that suggest higher solubilities than for metaluminous melts (Pichavant, Montel, and Richard, 1992; Montel, Mouchel, and Pichavant, 1988). Further experiments are being completed addressing apatite solubilities in a variety of granitic (s.l.) compositions (L.R. Richard, personal communication).

Harrison and Watson (1984) formulated their experimental results as a phosphorus Nernst partition coefficient. Recast as an empirical solubility expression (modified from 7 of Harrison and Watson, 1984) and solved for temperature, their results can be represented as

$$T = \frac{[26{,}400 \cdot C^{l}_{SiO_2} - 4{,}800]}{[12.4 \cdot C^{l}_{SiO_2} - \ln(C^{l}_{P_2O_5}) - 3.97]} \quad (1)$$

where T is the apatite saturation temperature (in kelvins), and $C^{l}_{SiO_2}$ and $C^{l}_{P_2O_5}$ represent the concentration of phosphorus and silica in the melt at the temperature at which apatite begins to crystallize ($C^{l,AST}_{SiO_2}$ and $C^{l,AST}_{P_2O_5}$ are expressed as weight fractions [wt percent/100]). Generally these values will not be the whole rock concentrations ($C^{l,o}_{SiO_2}$ and $C^{l,o}_{P_2O_5}$), except in those cases where apatite is a liquidus or near-liquidus phase. If apatite is the liquidus phase, the calculation of the temperature at which apatite begins to crystallize is straightforward given whole rock phosphorus and silica as estimators of $C^{l,AST}_{SiO_2}$ and $C^{l,AST}_{P_2O_5}$. Whereas this is not an unusual case in felsic melts, it is not true universally. The solubility of apatite is higher in more mafic magmas (for example, in a tonalite), and apatite may not appear until a third of the melt has crystallized. Therefore, before a model AST can be calculated for most intermediate to mafic melt compositions, the instantaneous concentration of P_2O_5 and SiO_2 as a function of progressive crystallization upon cooling must be estimated. There is no standard method by which these parameters can be estimated in felsic systems, and we therefore turn to experimental data to aid us in these estimations.

Melt Composition

Unfortunately, the difficult nature of cooling experiments of felsic magmatic compositions, especially in the water undersaturated region, has led to a paucity of precise and accurate data on crystallization progress and instantaneous melt composition as a function of temperature for felsic melts. To overcome this difficulty, data from several studies on the crystallization of felsic melts have been combined to yield a first order estimate of crystallization progress and instantaneous $C^{l}_{P_2O_5}$ and $C^{l}_{SiO_2}$ as a function of decreasing temperature at a pressure of 2 kb. This model, together with estimates of the initial magma composition ($Cl^{l,o}_{SiO_2}$ and $C^{l,o}_{P_2O_5}$) can be combined with eq (1) yielding: (1) the apatite saturation temperature (AST); (2) $C^{l,AST}_{SiO_2}$ at the point at which apatite begins to crystallize; and (3) the amount of apatite that has crystallized from the melt at a given temperature and $C^{l,o}_{SiO_2}$. Therefore, an understanding of the relationship between melt composition and temperature is critical.

The literature was searched for data on the relationships between melt composition, temperature, and the degree of crystallization at low pressures (0-4 kb). There is a large amount of these data available for mafic systems, both experimental (Juster, Grove, and Perfit, 1989; Luhr, 1990; Helz, 1976) and computational (Ghiorso, 1987; Ghiorso and Carmichael, 1987; Nekvasil, 1988a,b). Data of this type for felsic systems are sparse, due to the long times necessary to reach equilibrium in these systems. In a study by Johnson and Rutherford (1989), melt compositions were determined for experimental runs with Fish Canyon Tuff quartz-latite as the starting material (table 1).

TABLE 1

Whole rock analyses of samples used to estimate $C^{l,AST}_{SiO_2}$

Sample # Rock Name	101 Tonalite	1213 Tonalite	Fish Canyon Quartz-latite	R4 Granite	'Adamellite'
SiO_2	59.14	62.25	64.40	70.98	72.34
Al_2O_3	18.23	15.72	16.98	17.21	14.34
Fe_2O_3	2.32	1.03	n.a.	0.00	0.68
FeO	3.62	4.91	4.26	0.00	1.13
MgO	2.50	3.70	1.11	0.00	0.37
CaO	5.92	5.96	3.62	2.83	1.52
Na_2O	3.81	3.55	4.04	4.00	3.37
K_2O	2.19	1.67	4.06	5.07	5.97
H_2O^+	0.82	0.84	n.a.	0.00	$0.19^{(tot)}$
H_2O^-	0.04	0.03	n.a.	0.00	
TiO_2	0.79	0.69	0.60	0.00	0.26
P_2O_5	0.30	0.21	n.a.	0.00	0.11
MnO	0.11	0.11	0.11	0.00	0.02
A/CNK*	0.98	0.88	0.96	1.00	0.99
A/NK	2.11	2.06	1.54	1.43	1.19

Sources: (1) Cartridge Pass (101), Sierra Nevada Batholith (Piwinskii, 1968); (2) Needle Point Pluton (1213), Wallowa Batholith, Oregon (Piwinskii and Wyllie, 1967); (3) Fish Canyon Tuff (Johnson and Rutherford, 1989) represents the average of Fish Canyon Tuff analyses on an anhydrous basis, from table I; (4) (R4) Synthetic Granite (Whitney, 1975); (5) Adamellite, Westerly Granite (Whitney, 1988). A/CNK* is corrected for the P_2O_5 in apatite. n.a.—not analyzed.

Several older studies (prior to widespread use of electron beam microanalysis techniques) report crystallization progress, as well as $C^l_{SiO_2}$, as a function of temperature for rock melting experiments on a wide variety of natural starting materials. These studies, which use starting materials ranging from 59 to 77 wt percent SiO_2, are described in Piwinskii (1968) and Piwinskii and Wyllie (1967, 1970). The SiO_2 concentration in the glass fraction was determined in these experiments using the relationship, developed by George (1924), between the refractive index (n) of a natural glass and its SiO_2 content. George (1924) found that n decreased as the silica concentration in the natural glasses increased from 47 to 77 wt percent SiO_2. Piwinskii (1968) and Piwinskii and Wyllie (1967, 1970) used this relationship to determine the melt compositions for a variety of rock compositions.

Due to questions concerning the accuracy of this method, we decided to compare the silica concentrations determined by using the n method with those melt compositions determined by electron microprobe in the study of Johnson and Rutherford (1989) for the Fish Canyon Tuff. We chose to compare the 2 kb runs of tonalite 1213 from the Needle Point Pluton of the Wallowa Batholith (Piwinskii and Wyllie, 1967) with the 2 kb runs on quartz latites of the Fish Canyon Tuff (Johnson and Rutherford, 1989). The starting composition of tonalite 1213 is very similar to the Fish Canyon Tuff when compared on an anhydrous basis but with slightly different ratios of alkali metal oxides (table 1).

The results of the comparison between Johnson and Rutherford's measured $C^{l}_{SiO_2}$ and Piwinskii's estimates based on n can be seen in figure 1. The line on this figure is extracted from figure 14 of Piwinskii and Wyllie (1968) for their estimations of the melt compositions of their experiments using the n method. The data points are from figures 7 and 8 of Johnson and Rutherford (1989). These points represent 2 kb runs with f_{O_2} between NNO and MNO, the estimated f_{O_2} of the Fish Canyon Tuff. Runs at high temperatures (and therefore low crystallinity) with $X^{l}_{H_2O} \sim 1$ were removed because we wanted to model a magma that was vapor-undersaturated at low crystallinities. Likewise, runs at low temperatures (with high crystallinity) with low $X^{l}_{H_2O}$ were removed to simulate an approach to water saturation at lower temperatures. This is obviously crude, but the dearth of data concerning $C^{l}_{SiO_2}$ as a function of decreasing temperature leaves little choice. The fit between these two sets of experiments is extraordinary considering the method by which the $C^{l}_{SiO_2}$ were determined in the studies by Piwinskii and Wyllie.

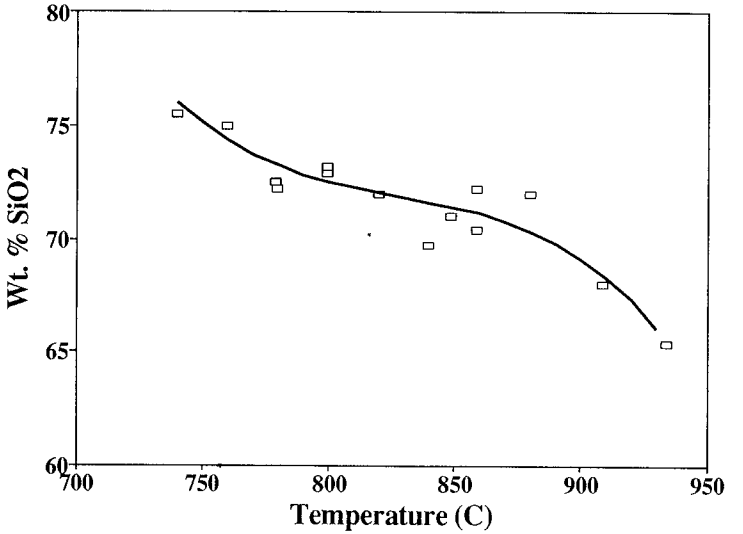

Fig. 1. Melt composition versus temperature. The line on the diagram was extracted from figure 14 of Piwinskii and Wyllie (1967; note scale change) from the tonalitic Needle Point Pluton of the Wallowa Mountain Batholith (sample 1213). Melt compositions in Piwinskii and Wyllie were determined using the refractive index technique described in George (1924). The data points are from experiments on the quartz-latitic Fish Canyon Tuff ($C^{l_o}_{SiO_2} = 64.40$; figs. 7 and 8) of Johnson and Rutherford (1989). These points represent 2 kb runs with f_{O_2} between NNO and MNO. Runs at high temperatures (and therefore low crystallinity) with $X^{l}_{H_2O} \sim 1$ were removed so as to model a magma that was vapor-undersaturated at low crystallinities. Likewise, runs at low temperatures (with high crystallinity) with low $X^{l}_{H_2O}$ were removed to simulate an approach to water saturation at lower temperatures.

The similarity of the estimates of $C^{l}_{SiO_2}$ using the n method and those determined by microprobe suggests that estimates of $C^{l}_{SiO_2}$ determined by the index of refraction method yield acceptable tentative estimates of how melt composition changes with temperature. We suggest that these data by Piwinskii (1968) and Piwinskii and Wyllie (1967, 1970) can tentatively be used to provide a first order estimate of melt composition with a variety of starting compositions (table 2). Given these assumptions, we can generate a series of equations that give $C^{l}_{SiO_2}$ for a given temperature for a variety of rock compositions of interest.

Unfortunately, these experiments do not give us information about how $C^{l}_{P_2O_5}$ changes with crystallization. If we make the assumption that apatite is the only phosphorus bearing phase (or modify the whole rock P_2O_5 according as described below) and assume that P_2O_5 is perfectly incompatible, the amount of phosphorus in the melt prior to the crystallization of apatite is given by the equation

$$C^{l}_{P_2O_5} = \frac{C^{l,o}_{P_2O_5}}{1 - X/100} \tag{2}$$

where $C^{l}_{P_2O_5}$ and $C^{l,o}_{P_2O_5}$ are the concentration of phosphorus in the melt and in the initial magma, respectively, and X is the crystallinity of the

TABLE 2

Sources of data to calculate $C^{l,AST}_{SiO_2}$, *T, and degree of crystallization*

Unit	% SiO_2	% Crystallization	References
Kuna Crest	tonalite 101	tonalite 101	1,1
Half Dome Equigranular	R4*	R4**	2,2
Half Dome Porphyry	R4***	R4**	2,2
Cathedral Peak	R4†	R4**	2,2
Johnson Porphyry	Westerly Granite‡	Westerly Granite‡	3,3

* The SiO_2 content was determined using the algorithm for the SiO_2 content of the Cathedral Peak, but was lowered by 3 wt percent due to the lower silica content of the Half Dome Equigranular.

** The relationship between percent crystallization and temperature was estimated using the contours from figure 2 of Whitney (1988) for a magma with 4 wt percent water in the original magma.

*** The SiO_2 content was estimated to be a linear function relative to the temperature between the whole rock composition and the ternary minimum at 2 kb.

† The $C^{l}_{SiO_2}$ for the Cathedral Peak was estimated to be a linear function relative to the temperature between the whole rock composition and the composition of the ternary minimum at 2 kb. The linearity of this has been previously suggested for high SiO_2 melts (see fig. 6, sample 104, Piwinskii, 1968).

‡ The $C^{l}_{SiO_2}$ was determined using a linear interpolation between the composition of the Johnson Porphyry ($C^{l,o}_{SiO_2} = 74.19$) and the minimum melt composition at 2 kb ($C^{l}_{SiO_2} \sim 78.7$). The effect of this on the determination of the AST is small due to the small difference in silica between the two compositions.

References: (1) Cartridge Pass, Sierra Nevada Batholith (Piwinskii, 1968), (2) Synthetic 'Adamellite' (Whitney, 1988), (3) Westerly Granite (Whitney, 1988).

magma. When combined with a suitable model for the variation in SiO_2, crystallization, and temperature, the following equation can be used to account for the crystallization of apatite in the subliquidus melt:

$$T = \frac{[26{,}400 \cdot C^{l}_{SiO_2} - 4{,}800]}{[12.4 \cdot C^{l}_{SiO_2} - \ln\left(\frac{C^{l,o}_{P_2O_5}}{1 - X/100}\right) - 3.97]}, \quad (3)$$

where $C^{l,o}_{P_2O_5}$ is the P_2O_5 concentration in the initial melt, and $C^{l}_{SiO_2}$ is the instantaneous SiO_2 concentration in the melt at apatite saturation. This equation can be solved for each magma composition of interest to determine the temperature, $C^{l}_{P_2O_5}$, and $C^{l}_{SiO_2}$ at which apatite becomes saturated in the melt.

Pressure

Pressure at epizonal levels does not have much effect on apatite/volatile phase equilibria due in part to the similarity of the molar volumes of the various apatite phase components ($\bar{V}^{o}_{ClAp}$ = 164,02, $\bar{V}^{o}_{FAp}$ = 157.53, and $\bar{V}^{o}_{HAp}$ = 158.22). Additionally, pressure has little effect on the solubility of apatite in melts under crustal conditions (Harrison and Watson, 1984). However, pressure does have an effect on the partitioning of chlorine between the magmatic volatile phase and melt and the speciation of chlorine in the magmatic volatile phase (Shinohara, Iiyama, and Matsuo, 1984 and 1989; Webster and Holloway, 1988; 1990), both of which affect the calculation of initial halogen concentrations in a melt. The pressure of formation can be obtained using various methods: (1) hornblende geobarometry as described by Hammarstrom and Zen (1986), Johnson and Rutherford (1989), and Schmidt (1992), (2) mineralogy of the igneous rocks (for example, presence of muscovite, minimum melt composition as a function of P_{H_2O}), (3) estimates from the mineral assemblage in the adjacent metamorphic rocks, et cetera. Ideally, one would estimate pressure so the dependence of chlorine speciation and concentration in the magmatic volatile phase could be determined.

CHLORINE AND WATER IN THE MAGMATIC VOLATILE PHASE AND THE MELT

Within the system $CaO–P_2O_5–H_2O–Cl_2O_{-1}$, given the phase components hydroxyapatite (HAp) and chlorapatite (ClAp) and the associated fluid containing HCl and H_2O, we can write the following condition of equilibrium

$$\mu^{Ap}_{Ca_5(PO_4)_3(OH)} + \mu^{aq}_{HCl} = \mu^{Ap}_{Ca_5(PO_4)_3(Cl)} + \mu^{aq}_{H_2O} \quad (4)$$

with the corresponding equilibrium constant

$$K_{(T,P)} = \frac{f^{aq}_{H_2O} \cdot a^{Ap}_{ClAp}}{f^{aq}_{HCl} \cdot a^{Ap}_{HAp}} = \frac{f^{aq}_{H_2O} \cdot X^{Ap}_{ClAp} \cdot \gamma^{Ap}_{ClAp}}{f^{aq}_{HCl} \cdot X^{Ap}_{HAp} \cdot \gamma^{Ap}_{HAp}} \quad (5)$$

where X^{Ap}_{ClAp} and X^{Ap}_{HAp} represent the mole fraction of chlorapatite and hydroxyapatite in apatite, respectively. Tacker and Stormer (1989) found that apatites mix nearly ideally (γ^{Ap}_{HAp} and $\gamma^{Ap}_{ClAp} = 1$) above 500°C and eq (5) can be reduced to

$$K_{(T,P)} = \frac{f^{aq}_{H_2O} \cdot X^{Ap}_{ClAp}}{f^{aq}_{HCl} \cdot X^{Ap}_{HAp}}. \quad (6)$$

If we calculate $K_{(T,P)}$ from thermodynamic data and determine the apatite composition, we can calculate $f^{aq}_{HCl}/f^{aq}_{H_2O}$. There is a large amount of thermodynamic data on the apatite endmembers in the literature. Tacker and Stormer (1989) address these data and the implications of the various values rather thoroughly. The thermodynamic data for apatite endmembers adopted here are from Zhu and Sverjensky (1991).

Equilibrium constants were calculated following the method of Perkins, Essene and Wall (1987). Input parameters used in the calculations that follow are (1) heat capacity, (2) Gibbs potentials of formation, (3) molar volume, and (4) molar entropy. $\Delta\mu^o$ of reaction at elevated T and P were calculated using

$$\Delta\mu^o_{P_2,T_2} = \Delta\mu^o_{P_1,T_1} + \sum_i v_i \cdot \int_{P_1}^{P_2} \overline{V}^o_i dP - \sum_i v_i \cdot \int_{T_1}^{T_2} \overline{S}^o_i dT \quad (7)$$

where

$$\int_{T_1}^{T_2} \overline{S}^o_i dT = \int_{T_1}^{T_2} \left[\overline{S}^o_{298} + \int_{298}^{T} \frac{\overline{C}^o_P}{T}\right] dT. \quad (8)$$

Using eqs (7) and (8) we can determine the equilibrium constants for a series of pressures and temperatures using the relationship $\Delta\mu^o = -RT\ln K$. The molar volume of the apatite species are very similar in magnitude (especially fluorapatite and hydroxyapatite), and because of this the pressure correction to the equilibrium constant (for example, eq 6) for apatite/volatile phase equilibria is rather small at low pressures. A fugacity formalism is used for H_2O, HCl, and HF, therefore obviating the need for a pressure correction for these phase components. An expression for the equilibrium constant given by eq (5) can be calculated as a function of temperature and pressure using the data in the caption associated with figure 2 and is given by

$$\mathrm{Log}_{10}\, K_{(T,P)} = 0.04661 + \frac{2535.8}{T} - \frac{0.0303 \cdot (P - 1)}{T} \quad (9)$$

where T is in kelvins, and P is in bars. The equation is valid over a temperature range of 873 to 1273 K (fig. 2). Progressive crystallization of apatite from a hypothetical melt with a constant ratio of f_{HCl}/f_{H_2O} with decreasing temperature will yield a rise in $X^{Ap}_{ClAp}/X^{Ap}_{HAp}$.

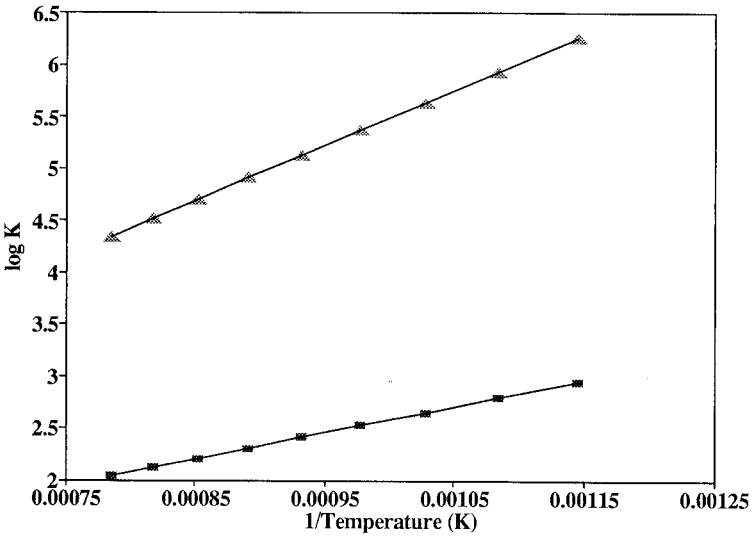

Fig. 2. Plot of the equilibrium constant for the reaction $\mu^{Ap}_{Ca_5(PO_4)_3(OH)} + \mu^{aq}_{HCl} \rightleftarrows \mu^{Ap}_{Ca_5(PO_4)_3(Cl)} + \mu^{aq}_{H_2O}$ (squares) and $\mu^{Ap}_{Ca_5(PO_4)_3(OH)} + \mu^{aq}_{HF} \rightleftarrows \mu^{Ap}_{Ca_5(PO_4)_3(F)} + \mu^{aq}_{H_2O}$ (triangles). Curves plotted at 1 bar. Thermodynamic data used to generate the curves are from the following sources: apatite endmembers, all data from Zhu and Sverjensky (1991); aqueous species from Robie, Hemingway, and Fisher (1979), with the exception of the heat capacity data for HF which is from Stull and Prophet (1971). Equilibrium constants were formulated using the method of Perkins, Essene, and Wall (1987).

Combining and rearranging eqs (6) and (9) yield an equation for the fugacity ratio as a function of apatite composition, T, and P:

$$\frac{f^{aq}_{HCl}}{f^{aq}_{H_2O}} = \frac{X^{Ap}_{ClAp}}{X^{Ap}_{HAp}} \cdot \frac{1}{10^{\left[0.04661 + \frac{2535.8}{T} - \frac{0.0303 \cdot (P-1)}{T}\right]}}. \qquad (10)$$

If the assumption can be made that a magmatic volatile phase was present at the AST, additional information can be obtained. Invoking the Lewis and Randall rule and assuming the ratio of the fugacity coefficients of HCl and H_2O is on the order of unity (information that does not exist at high T and P), the fugacity ratio can be set equal to the number of moles of HCl in the magmatic volatile phase (this step can be modified when data on mixing of H_2O and HCl at elevated T and P are available) yielding

$$m^{aq}_{HCl} \cong \frac{f^{aq}_{HCl} \cdot 1000}{f^{aq}_{H_2O} \cdot 18}. \qquad (11)$$

Combining eqs (10) and (11) yields

$$m^{aq}_{HCl} \cong \frac{X^{Ap}_{ClAp}}{X^{Ap}_{HAp}} \cdot \frac{1000}{18} \cdot \frac{1}{10^{\left[0.04661 + \frac{2535.8}{T} - \frac{0.0303 \cdot (P-1)}{T}\right]}} \qquad (12)$$

which gives the molality of HCl (but not the molality of Cl) in the magmatic volatile phase at the time apatite crystallized.

There is a limited amount of data that relates Cl complexed with H to total Cl ($C^{aq}_{\Sigma Cl} = C^{aq}_{HCl} + C^{aq}_{NaCl} + C^{aq}_{KCl} + 2C^{aq}_{FeCl_2}$, et cetera) in the magmatic volatile phase. The majority of the data that exist are from the work of Shinohara (ms), Shinohara, Iiyama, and Matsuo (1984, 1989), Urabe (1985, 1987), and Williams, Candela, and Piccoli (1991 and personal communication). Shinohara (ms) performed Cl and HCl partitioning experiments in the system SiO_2–Al_2O_3–K_2O–Na_2O–H_2O–Cl_2O_{-1} at 810°C, pressures between 0.6 and 6.7 kb, at a variety of aluminosities. The results of these experiments, as stated by Shinohara and discussed by Candela (1989a), suggest a pressure dependence on the ratio of HCl^{aq} to ΣCl^{aq}. The data of Shinohara (ms) are summarized in figure 3. The average $\log_{10}(HCl/\Sigma Cl)^{aq}$ for each of the pressures of Shinohara's ex-

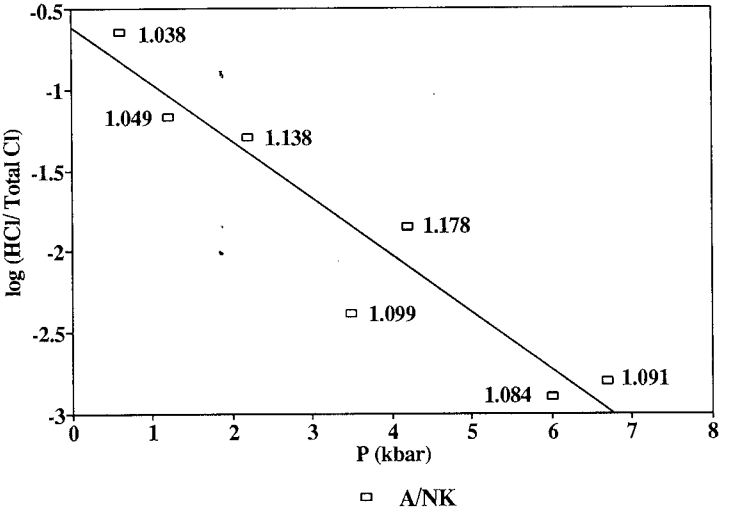

Fig. 3. Plot of the $\log_{10}(HCl/\Sigma Cl)^{aq}$ versus pressure of the experimental runs of Shinohara (ms). The line on the diagram represents a regression of the data and is described by the equation $\log_{10}(HCl/\Sigma Cl) = -0.631 - 0.354\,(P)$ [$r^2 = 0.90$]. The points on the diagram represent the averages of all Shinohara's runs at a given pressure, excluding all his data below minimum detection limit for HCl. The value in parentheses is the ASI (A/NK) of the experimental charge.

periments have been plotted along with the average ASI (Al_2O_3/(Na_2O + K_2O)) at each pressure.

Projecting along $\mu_{K(Na)_{-1}}$, $\mu_{H(Na)_{-1}}$ is a function of ASI. Urabe (1985) demonstrated that the aluminosity of a silicate melt has a strong influence on the quench pH in the system Na_2O–CaO–Al_2O_3–SiO_2–H_2O–Cl_2O_{-1}. In a more comprehensive set of experiments, Shinohara (ms) and Shinohara, Iiyama, and Matsuo (1984) found that the HCl concentration in the magmatic volatile phase increased as the Aluminum Saturation Index (ASI) of the melt increased in the system SiO_2–Al_2O_3–Na_2O_3 –K_2O–H_2O–Cl_2O_{-1}. The relationship between HCl in the magmatic volatile phase and melt composition, and its implications, have been discussed in detail in Candela (1990).

Within the hydrous, chloride-bearing metaluminous haplogranitic system $NaAlSi_3O_8$–SiO_2–KNa_{-1}–Cl_2O_{-1}–$AlO_{-1.5}$–HNa_{-1}, the equilibriagoverning $\mu_{H(Na)_{-1}}$ in the system can be represented at equilibrium by the chemical potential expression

$$\mu^{sys}_{H(Na)_{-1}} = \mu^{l}_{H(Na)_{-1}} \tag{13}$$

which can be written as

$$\tfrac{1}{2}\mu^{sys}_{H_2O} + \tfrac{1}{2}\mu^{l}_{Al_2O_3} + 3\mu^{l}_{SiO_2} = \mu^{sys}_{HNa_{-1}} + \mu^{l}_{NaAlSi_3O_8}. \tag{14}$$

The corresponding equilibrium is

$$K = \left[\frac{a^{sys}_{HNa_{-1}} \cdot a^{l}_{NaAlSi_3O_8}}{(a^{sys}_{H_2O})^{1/2} \cdot (a^{l}_{Al_2O_3})^{1/2} \cdot (a^{l}_{SiO_2})^{3}}\right] \tag{15}$$

In this expression, Al_2O_3 represents aluminum that is in excess of that needed to form normative feldspar (see Candela, 1990). More data on melt-volatile systems are needed to evaluate this equilibrum constant; however, the data of Shinohara can provide a reasonable estimate of (HCl/total Cl) for the purposes of this demonstration.

A regression of the averages of Shinohara's experimental results (0.6-6.7 kb) suggests that the HCl concentration can be related to the total Cl concentration in the magmatic volatile phase by the equation

$$\log (HCl/\Sigma Cl)^{aq} = -0.63 - 0.00035 \cdot P(bars). \tag{16}$$

The r^2 value for the regression of the averages is 0.90. It is important to note that the spread of the data in these experiments is up to $\pm$ 0.5 $\log_{10}$ units. These data suggest that a magmatic volatile phase in equilibrium with a magma at a depth of 1 km (0.3 kb) has about 20 percent of the Cl bound to H^+; at a depth of 6 km (2 kb) approximately 5 percent.

The starting compositions of the Shinohara experiments contain between 76 and 83 wt percent SiO_2. The runs, at 810°C and variable pressures, are at or near quartz saturation for the duration of these

experiments (however, the high pressure runs are above the liquidus). At 4 wt percent H_2O, quartz is probably the liquidus phase in these experiments. Therefore, the regression of the data from Shinohara (fig. 3) is strictly valid for modelling melts wherein $a^{l}_{SiO_2} = a^{l,QSAT}_{SiO_2}$. As will be discussed in the Tuolumne Intrusive Suite that follows, estimate of melt Cl and F can be adjusted to account for rocks that are not quartz-saturated when apatite begins to crystallize.

Combining eqs (12) and (16) we arrive at an equation for the concentration of Cl in the magmatic volatile phase in terms of apatite composition, temperature, and pressure,

$$m^{aq}_{Cl} = \frac{\frac{X^{Ap}_{ClAp}}{X^{Ap}_{HAp}} \cdot \frac{1000}{18} \cdot \frac{1}{10^{\left[0.04661 + \frac{2535.8}{T} - \frac{0.0303 \cdot (P-1)}{T}\right]}}}{10^{(-0.63 - 0.00035 \cdot P)}} \qquad (17)$$

which yields C^{aq}_{Cl} for metaluminous compositions. Addition of conversion factors yields the concentration of Cl in the magmatic volatile phase in ppm

$$C^{aq}_{Cl} = \frac{\frac{X^{Ap}_{ClAp}}{X^{Ap}_{HAp}} \cdot \frac{3.54 \times 10^7}{18} \cdot \frac{1}{10^{\left[0.04661 + \frac{2535.8}{T} - \frac{0.0303 \cdot (P-1)}{T}\right]}}}{10^{(-0.63 - 0.00035 \cdot P)}} \qquad (18)$$

as a function of apatite composition, pressure, and temperature. Using the definition of a Nernst-type partition coefficient ($D^{aq/l}_{Cl} = C^{aq}_{Cl}/C^{l}_{Cl}$), we can calculate the concentration of Cl in the melt (in ppm) that crystallized in equilibrium with apatite of this given composition at the AST:

$$C^{l}_{Cl} = \frac{\frac{X^{Ap}_{ClAp}}{X^{Ap}_{HAp}} \cdot \frac{3.54 \times 10^7}{18} \cdot \frac{1}{10^{\left[0.04661 + \frac{2535.8}{T} - \frac{0.0303 \cdot (P-1)}{T}\right]}}}{D^{aq/l}_{Cl} \cdot 10^{(-0.63 - 0.00035 \cdot P)}}. \qquad (19)$$

FLUORINE AND WATER IN THE MAGMATIC VOLATILE PHASE AND MELT

Within the system $CaO–P_2O_5–H_2O–F_2O_{-1}$, a parallel derivation can be completed for the concentration of F in the aqueous and melt phase,

with only minor changes. For a reaction with the phase components hydroxyapatite and fluorapatite and the associated fluid containing HF and H_2O, we can write the following condition of equilibrium

$$\mu^{Ap}_{Ca_5(PO_4)_3(OH)} + \mu^{aq}_{HF} = \mu^{Ap}_{Ca_5(PO_4)_3(F)} + \mu^{aq}_{H_2O} \tag{20}$$

with the associated equilibrium constant (and a statement accounting for ideality of apatite as described above)

$$K_{(T,P)} = \frac{f^{aq}_{H_2O} \cdot a^{Ap}_{FAp}}{f^{aq}_{HF} \cdot a^{Ap}_{HAp}} = \frac{f^{aq}_{H_2O} \cdot X^{Ap}_{FAp}}{f^{aq}_{HF} \cdot X^{Ap}_{HAp}}. \tag{21}$$

Incorporating the database listed in the caption of figure 2 into eqs (7) and (8), we arrive at an equation for the equilibrium constant in terms of T and P

$$\mathrm{Log}_{10}\, K_{(T,P)} = 0.18219 + \frac{5301.1}{T} - \frac{0.00360 \cdot (P - 1)}{T} \tag{22}$$

which is valid from 873 to 1273 K. The results are plotted in figure 2. As apatites crystallize from a melt that is buffered with respect to f_{HF}/f_{H_2O} with decreasing temperature, the ratio of $X^{Ap}_{FAp}/X^{Ap}_{HAp}$ will rise in the crystallizing apatite.

A series of steps similar to those used in the derivation of eqs (10) to (19) can be followed to arrive at equations for the concentration of F in the aqueous and melt phases. The speciation of F in the magmatic volatile phase has been calculated by Zhu and Sverjensky (1991) at 1 kb and a variety of temperatures. At magmatic temperatures, nearly all the F is present as HF and has therefore been neglected in this derivation.

The derivations for F in the magmatic volatile phase, parallel to the one above for Cl in eqs (10) to (19), yield

$$C^{aq}_F = \frac{X^{Ap}_{FAp}}{X^{Ap}_{HAp}} \cdot \frac{1.90 \times 10^7}{18} \cdot \frac{1}{10^{\left[0.18219 + \frac{5301.1}{T} - \frac{0.00360 \cdot (P-1)}{T}\right]}} \tag{23}$$

and

$$C^{l}_F = \frac{\frac{X^{Ap}_{FAp}}{X^{Ap}_{HAp}} \cdot \frac{1.90 \times 10^7}{18} \cdot \frac{1}{10^{\left[0.18219 + \frac{5301.1}{T} - \frac{0.00360 \cdot (P-1)}{T}\right]}}}{D^{aq/l}}. \tag{24}$$

THE VOLATILE/MELT PARTITIONING OF CL AND F

The concentrations of Cl, F, and OH in apatite are not independently variable but are related by the condition of closure $X^{Ap}_{ClAp} + X^{Ap}_{FAp} + X^{Ap}_{HAp} = 1$. The model presented here attempts to predict the initial Cl and F in the magma based on this relationship during second boiling (isobaric crystallization). However, we must first understand the behavior of the halogens in the magmatic volatile phase and the associated melt. Cl and F have been represented as having Nernst-type partitioning behavior between the magmatic volatile phase and melt (strictly, the Nernst Partition Coefficient is an empirical parameter that represents the cumulative effect of equilibria such as $NaCl^{aq} \rightleftharpoons NaCl^{l}$, $KCl^{aq} \rightleftharpoons KCl^{l}$, et cetera).

The partitioning of Cl between melts and a magmatic volatile phase appears to be complex. The work of Shinohara (ms), Shinohara, Iiyama, and Matsuo (1984, 1989), and Webster and Holloway (1988) suggests that $D^{aq/l}_{Cl}$ is a function of pressure. The data of Shinohara (ms) have been used here to model the behavior of $D^{aq/l}_{Cl}$. A regression of the metaluminous to slightly peraluminous ($0.98 < A/NK < 1.05$) haplogranitic melt data over the pressure range of 0.6 to 6.7 kb, at a temperature of 810°C was found to yield

$$D^{aq/l}_{Cl} = 3.75 + 19.8 \cdot P(kb) \tag{25}$$

($r^2 = 0.80$; $N = 63$; standard estimate of error of $D^{aq/l}_{Cl} \pm 17$). Webster and Holloway (1988) found that $D^{aq/l}_{Cl}$ decreases with decreasing temperature, as do C^{l}_{Cl}, P, and to a small degree, ASI for peraluminous-metaluminous magmas. Many of these experiments had high F concentrations, up to 7 wt percent, and these have therefore not been used. Detailed discussions of the behavior of $D^{aq/l}_{Cl}$ can be found in Candela (1989a), Webster and Holloway (1990), and Shinohara, Iiyama, and Matsuo (1989).

The partitioning behavior of fluorine between a magmatic volatile phase and a silicate melt has been studied by Dingwell and Scarfe (1983) on granitic systems. They report values for $D^{aq/l}_{F} = 0.2$ to 0.3. In addition, partition coefficients for F have also been obtained from experiments on the partitioning of F between a magmatic volatile phase and topaz rhyolite melts (Webster, 1990; Webster and Holloway, 1990). We have used the data of Webster (1990) from water-saturated experimental runs at 2 kb with <10,000 ppm F in the melt to derive a temperature dependent partition coefficient:

$$D^{aq/l}_{F} = -0.56 + 0.00093 \cdot T(°C) \tag{26}$$

($r^2 = 0.92$; $N = 7$; standard estimate of error of $D^{aq/l}_{F} \pm 0.028$). Webster and Holloway (1990), however, noted increasing $D^{aq/l}_{F}$ with decreasing temperatures in melts with 7500 to 68,000 ppm F. At this time, it is not clear whether there is a pressure dependency on $D^{aq/l}_{F}$. Both determinations of $D^{aq/l}_{F}$, our modification of Webster's data and those of Dingwell and Scarfe will be used in our calculations below.

ASSUMPTIONS

Original Magma was Entirely Melt

The MASH model for Andean magmatism (Hildreth and Moorbath, 1988) provides a framework for a discussion of the origin of magma in arc systems. They considered the arc magmas of the central Chilean Andes to have acquired base-level geochemical signatures within zones of melting, assimilation, storage, and homogenization (MASH) near the base of the crust. There, a basaltic mantle (wedge + slab) component mixes intimately with deep crustal material to yield melts with a range of compositions (for example, tonalitic to granitic plutons of the Tuolumne Intrusive Suite: example 2 that follows). Our working model is that the plutons we now sample in the Tuolumne Intrusive Suite were extracted as mostly molten magma batches from a MASH-like zone. The modelling of Kistler and others (1986) suggests that the magmas that gave rise to the Tuolumne Intrusive Suite plutons were hybrids of mantle-derived and crustal melts. If phenocrysts (for example, plagioclase) were carried from this zone, no error would be introduced into the calculations presented here, as any material carried with the melt would represent material crystallized at a higher temperature.

Source rock inclusions, high-anorthite plagioclase cores, and inherited zircons are features often used as evidence for the restite model. Inclusions alone do not suggest restite unmixing occurred (Barbarin, 1991), although many enclaves have been interpreted as representing restite (Chappell and White, 1991). Although there are cases in which it can be determined the restitic material is present, demonstrating the absence of restite is more difficult. The presence of restitic material in a melt *may* produce errant estimates of AST's either as over- or underestimates of the actual temperature at which apatite begins to crystallize (and therefore possibly errant estimates of $C_{Cl}^{l,o}$ and $C_{F}^{l,o}$). Caution should therefore be used when attempting to apply eq (1) (or eq 1 could be modified to account for restite component).

Apatite Does Not Exchange Halogens with Adjacent Crystals

Apatites are generally present in a variety of petrographic associations in plutonic and volcanic rocks; adjacent to or included within quartz, K-feldspar, plagioclase, biotite, amphibole, and opaque phases. The potential exists for subsolidus exchange to occur between apatite and other halogen-bearing minerals (for example, biotite, hornblende, et cetera). The potential for exchange suggests that only apatite associated with anhydrous phases should be analyzed (as was done in this study) so that this potential exchange is avoided.

Alteration Does Not Change Halogen Concentrations in Apatite

It has been suggested that halogen-bearing minerals may change composition during hydrothermal alteration or upon interaction with meteoric water as plutons rise toward the surface. This is thought to be a minor problem with volcanic rocks, due to the rapid rate at which they

cool. In plutonic rocks, instances may exist where subsequent modification of halogen-bearing phases could take place. Experimental evidence suggests that apatite is fairly resistant to resetting of halogens at submagmatic temperatures. Although the time scales in these experiments are short compared to natural systems, apatite appears to be less susceptible to hydrothermal resetting than many minerals used in geothermometry and geobarometry. Ekstrom (1973) and Latil and Maury (1977) found that re-equilibration of apatite is sluggish at temperatures below 500° to 600°C. Further, Elliott and Young (1973) found that chlorapatite only partially re-equilibrates with an H_2O-rich gaseous phase at 1300°C.

For natural suites of rocks, isotopic systematics may be useful in determining whether alteration has taken place. Creaser and Gray (1992) show that $(^{87}Sr/^{86}Sr)_i$ in apatite from hydrothermally altered granitic and volcanic rocks is not altered significantly as a result of igneous cooling or hydrothermal alteration even though whole rock $(^{87}Sr/^{86}Sr)_i$ was extensively modified. In fact, Creaser and Gray suggest that $(^{87}Sr/^{86}Sr)_i$ may be obtained from apatite in the hydrothermally altered rocks they studied.

Zoning

It is possible that diffusion of halogens within apatite occurs during the protracted cooling history of igneous plutons, obliterating primary zonation. However, apatite zonation (with respect to halogens) is found in neither felsic volcanic rocks nor their plutonic equivalents. On the other hand, hydrothermal apatites are commonly zoned (for example, Roegge and others, 1974). The lack of zoning in volcanic apatites suggests that the lack of zoning in plutonic apatites is *not* due to subsolidus homogenization during slow cooling.

LIMITATIONS OF THE MODEL

Crystallization of apatite at temperatures below the AST.— The determination of the AST described above represents the temperature at which apatite *begins* to crystallize. Apatite will continue to crystallize until the magma reaches the solidus. What then is the significance of the AST for the actual temperatures of apatite crystallization? The volume of apatite that crystallizes over a specific temperature range can be calculated using a modified version of eq [1]. As a general rule, the majority of the volume proportion of apatite crystallizes within approx 60°C of the AST in granodioritic to quartz-dioritic magmas, and within 30°C of the AST for granite magmas (fig. 4), and the AST can be used to make initial estimates of the temperature at which the majority of the apatite crystallizes. Conversely, a large portion of the aluminosilicate minerals crystallize within a small temperature interval near the solidus. Therefore, the lack of any electron probe-resolvable zoning in apatite is due to the small temperature range over which most of the volume of apatite crystallizes.

Phosphorus in silicates and phosphates.—Three approaches can be taken to estimate P_2O_5 for the calculation of the AST. P_2O_5 can be calculated by using: (1) whole-rock P_2O_5 to calculate the AST (that is,

make the assumption that all the P_2O_5 is present in the rock in the mineral apatite), (2) whole-rock P_2O_5 minus the P_2O_5 in phases other than apatite (estimated by using published partition coefficients), and (3) the amount of P_2O_5 that is in the mineral apatite only.

The calculation of AST's that use uncorrected whole rock P_2O_5 (approach 1) yields the highest temperatures of the 3 methods described when solving eqs [1] and [3]. However, if a calculation is made to determine the maximum modal amount of apatite that could be present given the whole-rock P_2O_5, this method is found to overestimate P_2O_5 by twice the amount estimated using point-counting methods. This suggests that P_2O_5 is present as either phosphorus-bearing phases or substituting into silicate phases.

We can make a general statement about the amount of P_2O_5 that is being incorporated into apatite and other P-bearing phases if these minerals crystallize simultaneously. The effect of crystallization of REE-phosphates (for example, monazite- 30 wt percent P_2O_5) on melt P_2O_5 is generally small because the ratio of the weight of P_2O_5 to total weight in REE-phosphates is small, and apatite is therefore still the main phosphorus sink in the rocks. If the mode of these phases becomes $\gg$ apatite, the error in this estimation becomes large, and approach 3 should be taken.

The partitioning of phosphorus into feldspars and quartz has been addressed by London (1990) and London, Loomis, and Huang (1990) and London and others (1990). $D^{x1/1}_{P_2O_5}$ was determined to be 0.25–0.35 for metaluminous magmas near water saturation at 750°C.

The partitioning of phosphorus into plagioclase was found to be two-thirds of that in alkali feldspar. Although temperature appears to have a minor effect on the partitioning of phosphorus into feldspars, the aluminum saturation index has a large effect; the partition coefficient rises to 1 as the ASI approaches 1.4 (London, personal communication). Micas, amphiboles, and zircons may also incorporate significant quantities of phosphorus.

In our opinion, the best method to determine the P_2O_5 content at the AST is to obtain a high precision modal count of apatite and calculate the amount of P_2O_5 contained in apatite. These modal analyses can be performed either by standard point counting techniques on a large number of points or by using an electron microprobe which can analyze a large number of points in a relatively short period of time.

The estimation of AST as calculated here is dependent upon the mode of apatite. Traditional modal analyses of thin sections may not be accurate enough for the purposes described here due to the low proportion of apatite in many rocks. A logical solution is to use an electron probe for the modal proportion of apatite, which is a relatively simple procedure. Approx 65,000 points can be analyzed for the presence or absence of apatite in fractions of an hour. The accuracy of the modes determined by this method has the potential to be much more accurate than traditional optical methods.

Aluminum saturation index.—The calculation as presented here is designed to be used when modeling felsic, metaluminous rocks which yield a magmatic volatile phase due to second boiling. However, behavior of the solubility of apatite, speciation of Cl in the magmatic volatile phase, Cl partitioning between the magmatic volatile phase and the melt, and crystallization of accessory phases are drastically different in peralkaline and peraluminous systems. The experimental database is currently not large enough to be able to address these problems readily.

EXAMPLE 1: PLINIAN PHASE OF THE BISHOP TUFF

The Bishop Tuff is a 700 Ka, large-volume rhyolite thought to have been erupted quickly (forming the Long Valley Caldera) and abruptly quenched upon eruption. It consists of two stratigraphic units: (1) an initial basal plinian air-fall tuff (PBT), exhibiting minor compositional zoning (Gardner, Sigurdsson, and Carey, 1991) and containing Fe-Ti oxides which yield low and restricted temperatures of equilibration (720°-725°C; Hildreth, 1979), and (2) secondary ash-flow sheets which yield Fe-Ti oxide temperatures of 723° to 790°C. Based on water and carbon dioxide solubility studies, Anderson and others (1989) suggest pressures of 1.6 kb for the magma chamber that erupted the PBT.

We chose to model apatite crystallization from the PBT for two reasons: (1) there is a significant amount of data on the halogen content of melt inclusions from within the air-fall sequence, which provides a useful comparison to the calculations attempted here based on apatite chemistry, and (2) the Fe-Ti oxide temperature range over which these rocks were erupted is restricted, and therefore the plinian phase is thought to have cooled more quickly than the ash-flow tuffs that remain hot for a longer period of time.

Determination of Apatite Saturation Temperatures and Initial Halogen Concentrations

As described above, the experimental work of Harrison and Watson (1984) suggests that $C^l_{SiO_2}$ and $C^l_{P_2O_5}$ are the two most important parameters in determining the temperature at which apatite begins to crystallize in metaluminous, felsic magmas. The PBT contains 77.16 wt percent SiO_2 (N = 13, $1\sigma = \pm 0.46$ (sample standard deviation of whole rock analyses)), 0.03 wt percent P_2O_5 (N = 13, $1\sigma = \pm 0.01$) (12 samples from Gardner, Sigurdsson, and Carey, 1991, and sample B-104 from Hildreth, ms), and is metaluminous (A/CNK = 1.00; A/NK = 1.11). As described above, the whole rock SiO_2 can be adjusted so that $C^l_{SiO_2}$ can be estimated as crystallization proceeds. The whole rock SiO_2 (77 wt percent) is close to the minimum melt $C^l_{SiO_2}$ at 1.6 kb ($C^l_{SiO_2} \sim 78$), and therefore it has been treated as increasing in silica linearly throughout crystallization in this example. This treatment is supported by experimental evidence from high silica experimental runs which suggest that melt composition varies linearly with crystallization at high silica contents (for

example, sample 104, Piwinskii, 1968; for a discussion, see Bergantz, 1990).

The lack of phosphorus-bearing phases other than apatite in the PBT allows the use of the amount of P_2O_5 found in apatite as an estimator of whole rock P_2O_5, that is, we assume that all the P_2O_5 is present in apatite. Although this simplification is not strictly correct (a small amount of P_2O_5 will be included in feldspars, zircon, et cetera), it is thought to be a good estimation due to the small amounts of crystals in the PBT (5-10 percent, Anderson and others, 1989) and the low solubility of apatite in metaluminous, high-silica melts. The error induced by making this assumption is thought to be small. However, the AST calculated using this method will represent a maximum, and the estimates of initial halogen concentrations will also be a maximum. Additionally, the largest volume of apatite that crystallizes from the PBT melt should crystallize within a small ΔT below the AST (this effect will be discussed in detail in the following example).

The AST calculated in this manner for the PBT is 860°C using unmodified whole rock P_2O_5. The calculation suggests that the AST is reached after only a small degree of crystallization. The $C^{l,AST}_{SiO_2}$ and $C^{l,AST}_{P_2O_5}$ in this case are nearly equal to the initial silica and phosphorus content of the melt, due to the high silica content of the rock (SiO_2 close to the minimum melt) and the small amount of crystallization that has taken place.

This AST has been used in conjunction with four apatite analyses from the PBT (listed in table 3; from table 17 of Hildreth, ms) and eqs (18), (19), (23), and (24) to calculate the concentrations of Cl and F in the magmatic volatile phase and the melt at the AST. The magmatic volatile phase is estimated to contain 31,000 to 42,000 ppm Cl (0.05 molal HCl or 1.2 molal Cl) and 160 to 300 ppm F (0.003 molal F) when the calculations are performed in the manner described above. These values correspond to 700 to 960 ppm Cl and 160 to 300 ppm F in the melt (table 3). Due to the small amount of crystallization in the PBT (5-10 volume percent, Anderson and others, 1989), it is thought that $C^{l,AST}_{Cl} = C^{l,o}_{Cl}$ and $C^{l,AST}_{p} = C^{l,o}_{p}$, and the initial values have therefore not been calculated.

Discussion

A series of studies of the PBT has been completed in which melt inclusions have been analyzed (see table 3). Anderson and others (1988 and 1989) using electron probe analyses report Cl concentrations of 600 to 800 ppm Cl for melt inclusions in quartz (except for hourglass-shaped inclusions which yield values of 300 ppm Cl and which the authors interpret to represent effervescence prior to or during eruption). Furthermore, Dunbar and Hervig (1990a,b, 1992) analyzed melt inclusions in a variety of phenocrysts within the PBT and report melt Cl concentrations, generally in the range 600 to 900 ppm. Estimates of C^{l}_{Cl} based on apatite chemistry are similar to these measured Cl values in melt inclusions. This suggests that the technique may have reasonable potential in estimating

TABLE 3

Bishop Tuff apatite analyses and estimates of initial halogen concentrations

Sample	B-93	B-98	B-104	B-110	Melt Inclusions
Wt % Cl in Apatite	0.20	0.22	0.21	0.24	
Wt % F in Apatite	3.00	2.78	2.71	2.82	
X^{Ap}_{ClAp}	0.03	0.03	0.03	0.04	
X^{Ap}_{FAp}	0.80	0.74	0.72	0.75	
C^{aq}_{Cl}	42,000	35,000	31,000	40,000	
C^{l}_{Cl}	960	800	700	930	600–900
C^{aq}_{F}	60	42	38	45	
$C^{l(1)}_{F}$	300	210	190	230	250–700
$C^{l(2)}_{F}$	260	180	160	200	

All concentrations are in ppm. Values for C^{l}_{Cl} were calculated using the $D^{aq/l}_{Cl}$ described in the text. Values for C^{l}_{F} were calculated using the $D^{aq/l}_{F}$ from (1) Dingwell and Scarfe (1983) and (2) estimated from the data from table 3 of Webster and Holloway (1990) for water saturated melts with less than 10,000 ppm F at 2 kb. Melt inclusion data: Values for C^{l}_{Cl} from the melt inclusions within the plinian phase of the Bishop Tuff are from five sources: (1) Anderson and others (1989) who report values of 600 to 800 ppm; (2) Dunbar and Hervig (1990b) who report values of 800 to 900 ppm; (3) Dunbar and Hervig (1990a) who report values of 700 to 900 ppm; (4) Dunbar and Hervig (1992) who report 39 analyses, the majority of which range between 600 to 900 ppm; and (5) Anderson and others (1988) who report 700 ppm for most inclusions. Values for C^{l}_{F} in melt inclusions are from 3 sources: (1) Dunbar and Hervig (1992) who report 62 analyses, the majority of which are in the range of 300 to 700 ppm; (2) Dunbar and Hervig (1990b) and represents the average of four values, 560, 580, 460, and 490; and (3) Fangqiong Lu (personal communication) who has 65 analyses which range from 246 to 480 ppm F. The apatite analyses from the Plinian Phase of the Bishop Tuff are from Hildreth (ms, table 17). The whole rock data used to make estimates of AST are from Hildreth (ms) and Gardner, Sigurdsson, and Carey (1991). The AST estimate is 860°C. The pressure estimate used in the calculation is 1.6 kb, as described in Anderson and others (1989). The melts are nearly saturated with respect to apatite upon intrusion. We do not calculate $C^{l,o}_{Cl}$ and assume it to be equal to $C^{l,AST}_{Cl}$ within error. X^{Ap}_{ClAp} was calculated using wt percent Cl in apatite/6.809. Similarly, X^{Ap}_{FAp} = wt percent F in apatite/3.767.

halogen concentrations in melts if, in fact, melt inclusions are representative of melt compositions. The estimated C^{l}_{Cl} using apatite (700-960 ppm) are higher than measurements of whole rock Cl (280-670 ppm, Hildreth, 1981). This is consistent with the loss of a volatile phase, which would contain significant Cl, upon rise of the PBT to the surface.

Similarly, melt inclusions have been analyzed for F in the Plinian phase. Dunbar and Hervig (1990b, 1992) report 66 analyses, the majority of which are in the range 300 to 700 ppm F. Fangqiong Lu of the University of Chicago (personal communication, 1990) analyzed 65 melt inclusions for F and found a range of 246 to 480 ppm. Estimates of C^{l}_{F} (160-300 ppm) are somewhat lower than both sets of values for melt inclusions (246-700 ppm) and whole rock values (340-560 ppm; Hildreth, 1981). This 'apparent' underestimation of melt F may occur for 2 reasons: (1) the majority of the data on $D^{aq/l}_{F}$ were determined using

peraluminous and not metaluminous melts, and (2) estimates are based on the assumption that F present in the magmatic volatile phase is present complexed to hydrogen (that is, not AlF_3, et cetera) which is supported by calculations by Zhu and Sverjensky (1991). Overall, this technique appears to be promising in estimating halogen concentrations of the PBT.

Water contents in melt inclusions have been measured in the PBT. Anderson and others (1989) report an average value of 5.7 wt percent H_2O^{TOT} based on water and carbon dioxide solubility studies, similar to other recorded values (Dunbar and Hervig, 1990a,b; Anderson and others, 1988; Anderson and others, 1989; Skirius and Anderson, 1988). When used in conjunction with estimates of C^l_{Cl} based on apatite chemistry, the $C^l_{Cl}/C^l_{H_2O}$ ranges from 0.012 to 0.017, values nearly equal to the Cl/H_2O ratios measured in melt inclusions (0.010-0.016).

Gill (1981) reports and discusses Cl/H_2O in andesites and basalts from a variety of sources, including volcanic gases, leachates, lavas, and glass inclusion measurements, and reports values of 0.1 to 0.028. The values of the PBT estimated using apatite chemistry are half to one-tenth of the values reported in Gill (1981). The reasons for this difference may be that the systems considered by Gill, (that is, oceanic and continental arcs) contain a higher subcrustal component than the PBT.

Upon first glance, AST's of 860°C may seem rather high. Fe-Ti oxides yield equilibration temperatures approximately 135°C lower. The temperature of 860°C is close to the low pressure, water-saturated liquidus temperature for a rock of this composition (see the 2 kb runs of Piwinskii and Wyllie, 1970, sample 104). Petrographically, most apatite occurs poikilitically enclosed within other phases in the Bishop Tuff (especially pyroxene), but microphenocrystic apatite grains do occur. Few apatite grains are thought to be cognate (Hildreth, ms), and the estimates of AST and initial halogen estimations are therefore maximum. Our estimates that apatite crystallized prior to the Fe-Ti oxides are consistent with the findings of Hildreth (ms, p. 24) who reports the following sequence of crystallization: pyrrhotite, apatite, zircon, Fe-Ti oxides, followed by the silicates.

The crystallization of phases, other than apatite, that incorporate significant amounts of phosphorus and are present in significant quantities, will have the effect of lowering estimates of the AST. Zircon, the only other phase that incorporates significant amounts of P_2O_5 in the PBT should not have an effect on the calculated AST for two reasons: (1) zircons from the PBT contain approx 0.30 wt percent P_2O_5 (Hildreth, ms, table 16), over two orders of magnitude less than that of apatite (−42 wt percent), and zircon would have to be present in concentrations 100 times greater than apatite to incorporate similar amounts of melt P_2O_5, and more importantly (2) zircon appears after apatite in the crystallization sequence and therefore should have no effect on the calculated AST.

This example serves as a useful model calculation because the effect of apatite chemistry on estimations of initial halogen concentrations can

be demonstrated easily due to the fact that the PBT has been modeled as having one AST. A single AST was calculated for the PBT, whereas apatite analyses from four sample sites have been used in this estimation. The whole rock sample sites (mostly from Gardner, Sigurdsson, and Carey, 1991) and apatite sample sites (from Hildreth, ms) could not be cross-correlated; however, all are from the PBT. The PBT is relatively homogeneous with respect to whole-rock composition, and this should allow for this comparison within the error of this type of calculation. As would be expected, the apatite with the highest X^{Ap}_{FAp} (0.80; B-93; table 3) yields the highest estimates of F concentrations (260-300 ppm). However, this same sample, with low X^{Ap}_{ClAp} (0.03), yields the highest estimates of magmatic Cl. The reason for this is apparent when looking at eqs (18) and (19): the equations for C^{aq}_{Cl} and C^{l}_{Cl} as derived here are dependent not only upon the X^{Ap}_{ClAp} but also X^{Ap}_{HAp} (see fig. 2). The lower the X^{Ap}_{HAp}, the greater the apparent C^{l}_{Cl}. Thus, the sample with the highest estimates of magmatic Cl (yet the lowest X^{Ap}_{ClAp}), as expected, has the lowest X^{Ap}_{HAp}. This emphasizes the importance of obtaining good Cl and F determinations in apatite.

EXAMPLE 2: TUOLUMNE INTRUSIVE SUITE

The Tuolumne Intrusive Suite (TIS) is a concentrically zoned intrusion in the Sierra Nevada Batholith. The granitic rocks that make up the suite are progressively younger and more felsic toward the interior. The rim of the TIS is granodioritic-quartz dioritic (Kuna Crest: KC), with an intermediate granodioritic portion (Half Dome Equigranular: HDE, Half Dome Porphyry: HDP, and Cathedral Peak: CP) and a core that is granitic in composition (Johnson Porphyry: JP). Rocks described in this study have been collected along the western portion of the traverse described in Bateman and Chappell (1979) and Bateman and others (1988). These rocks have been described in detail by Bateman and Chappell (1979), Bateman (1988), Kistler and others (1986), and Reid, Evans, and Fates (1983). It has been suggested by some workers (for example, Bateman and Chappell, 1979) that a discrete water-rich phase was present during a considerable portion of the crystallization of these rocks. Hornblende geobarometry suggests that these rocks crystallized at about 2 kb (Piccoli, ms) which is consistent with the metamorphic grade in the surrounding country rocks. The mineralogy present in these rocks does not allow for estimates of crystallization temperatures using Fe-Ti oxides.

Determination of Apatite Saturation Temperatures and Initial Halogen Concentrations

As described above, $C^{l}_{SiO_2}$ and $C^{l}_{P_2O_5}$ are the two most important factors in determining the temperature at which apatite saturates in a melt. The Tuolumne Intrusive Series exhibits a 15 percent variation in SiO_2 across the pluton (table 4), and the $C^{l}_{SiO_2}$ at which apatite begins to crystallize will be different in each of the units in the TIS due to this variation in SiO_2.

TABLE 4

Composition of the Tuolumne Intrusive Suite

Unit	KC(4)	HDE(7)	HDP(2)	CP(7)	JP(2)
SiO_2	58.7	66.8	67.8	69.7	74.2
Al_2O_3	16.8	15.2	15.5	15.3	13.7
Fe_2O_3	2.30	1.71	1.53	1.25	0.69
FeO	4.17	2.09	1.42	1.06	0.47
MgO	3.22	1.59	1.06	0.71	0.23
CaO	6.20	3.71	3.31	2.70	1.24
Na_2O	3.55	3.53	3.96	4.30	3.58
K_2O	2.19	3.59	3.67	3.55	4.75
H_2O^+	1.21	0.69	0.57	0.52	0.53
H_2O^-	0.18	0.13	0.12	0.12	0.13
TiO_2	0.87	0.51	0.48	0.39	0.15
P_2O_5	0.21	0.16	0.17	0.14	0.03
MnO	0.11	0.08	0.06	0.05	0.04
A/CNK*	0.88	0.93	0.94	0.98	1.04
A/NK	2.05	1.57	1.48	1.40	1.25
$(^{87}Sr/^{86}Sr)_i$(87 my)	0.7059	0.7061	0.7064	0.7064	0.7066
$\epsilon_{Nd}(T)$	−3.5	−5.3	N.A.	−5.7	−8.0

Analyses are from Bateman and others (1988) and represent the averages of western portion of their traverse. Number in parentheses represents the number of analyses included. Abbreviations are as follows: KC–Kuna Crest, HDE–Half Dome Equigranular, HDP–Half Dome Porphyry, CP–Cathedral Peak, JP–Johnson Porphyry. $(^{87}Sr/^{66}Sr)_i$(87 my) and $\epsilon_{Nd}(T)$ are from tables 1 and 3 of Kistler and others (1986) and represent average values from the western portion of the traverse described in that text. A/CNK* is corrected for the P_2O_5 in apatite.

The assumption has been made that the composition of the rocks from the TIS represent the composition of the original magma in which they crystallized, as may be the case in rocks formed due to magma mixing (as was described by Kistler and others, 1986, for the rocks of the TIS). A comparison of the compositions of units of the TIS (table 4) with the experiments from which melt compositions have been determined (table 1) allows us to pick experiments that will be used to simulate crystallization of each of these plutons. The samples chosen for this comparison and the parameters used in this calculation can be found in table 2.

The adjustment of whole rock SiO_2 to estimate $C^{l,AST}_{SiO_2}$ is critical for the more mafic rocks; however, a smaller effect is expected for the more silicic rocks (as in the PBT example). We chose to calculate a temperature-composition path for the Kuna Crest granodiorite (the most mafic unit in the TIS) by using the crystallization data for tonalite 101 of Piwinskii (1968). The $C^{l}_{SiO_2}$ and crystallinity of the tonalite of Piwinskii and the KC were regressed with a second order function, against temperature. The tonalite of Piwinskii and the KC are close in composition (< 1 wt percent difference in SiO_2). It is critical that the most mafic units in the suites have analogues very similar in composition, because it is in these rocks that crystallization will proceed to a significant degree before apatite saturation.

The matching of compositions of the intermediate units in the TIS (HDE, HDP, and CP) with experimental analogues is not as critical as with the KC because the composition of the melt in which apatites begin to crystallize in these rocks is much closer to the composition of the initial magma. The data of Whitney (1988; synthetic granite R4, estimated from the contours on fig. 2), were used assuming $C^{l,o}_{H_2O}$ = 4 wt percent to estimate crystallinity as a function of temperature. The same crystallinity function was used for all the intermediate units of the TIS. The $C^{l}_{SiO_2}$ for each of the units was treated as though the effect of changing temperature was linear. A linear trend between $C^{l}_{SiO_2}$ and temperature is evident in the more silicic experiments of high silica systems (sample 104, fig. 6, Piwinskii, 1968) where the dominant minerals crystallizing are quartz, K-feldspar, and plagioclase. This trend has been modeled as a linear combination of the crystallization trends for synthetic granite R4 ($C^{l,o}_{SiO_2}$ = 70.98) and the minimum melt composition at 2 kb ($C^{l}_{SiO_2} \cong 78$). The $C^{l}_{SiO_2}$ calculated using this algorithm were lowered relative to the minimum melt, by a factor of 1, 3, and 4 wt percent SiO_2 for the HDE, HDP, and CP, respectively, due to their lower whole-rock SiO_2 content.

We chose to model the core of the TIS, the Johnson Granite Porphyry, with the Westerly granite ('Adamellite') of Whitney (1988). A linear interpolation was utilized to estimate the melt composition between the whole-rock SiO_2 of the JP (74.2 wt percent) and the minimum melt compositions, similar to that described above.

The foregoing procedure, utilizing experimental data on the relationships among melt composition, temperature, and crystallinity, allows us to calculate the $C^{l}_{P_2O_5}$ and $C^{l}_{SiO_2}$ at any temperature below the liquidus. We then checked for apatite saturation at sufficiently small temperature intervals using the data of Harrison and Watson (1984).

Three approaches were taken to determine AST values for the units of the TIS: (1) all the whole-rock P_2O_5 was assumed to be consumed in the formation of apatite, (2) the whole-rock P_2O_5 was modified to account for phosphorus in feldspars, and (3) whole-rock P_2O_5 was estimated from modal analyses of apatite.

Calculations of the AST using unadjusted whole-rock P_2O_5 yield the highest temperatures and $C^{l,AST}_{P_2O_5}$ at which the melts saturate with respect to apatite and the lowest $C^{l,AST}_{SiO_2}$ and degree of crystallization of any of the three methods described. The highest AST's calculated using this approach are in the units midway between the core and the rim of the suite (HDP-965°C and CP-964°C), whereas the lowest AST is found in the core (JP-834°C). Estimation of $C^{l,AST}_{P_2O_5}$ using this method is inaccurate due to P_2O_5 being incorporated into silicates and phosphates other than apatite (monazite).

The application of method 2 requires either the measurement of P_2O_5 in minerals other than apatite or the determination of experimental

partition coefficients. Studies of feldspars from both natural (London, 1990; London and others, 1990; Kontak and Strong, 1988) and experimental (London, Loomis, and Huang, 1990) systems suggest that a significant amount of P_2O_5 can be incorporated into K-feldspar and plagioclase feldspar, via the berlinite substitution ($AlPSi^{4+}_{-2}$). Within each of the cases they studied, the P_2O_5 content of the feldspars increased with progressive crystallization. To monitor the effect of phosphorus substitution into silicates on the AST, we chose to use a Rayleigh fractionation model for the removal of phosphorus into feldspars from the melt. The values $D^{AF/l}_{P_2O_5} = 0.3$ and $D^{PL/l}_{P_2O_5} = 0.2$ (London, Loomis, and Huang, 1990) and the modes of the feldspars were used for each of the units in the TIS. The AST's calculated in this manner accounting for P_2O_5 in silicates are only on the order of 2°C lower than those we calculated using the whole rock P_2O_5. Although the amount of phosphorus in feldspars can be significant (especially in highly peraluminous rocks), the effect of this on the AST is small due to the small amount of crystallization that occurs prior to the AST.

The third approach in determining $C^{l}_{P_2O_5}$ for the calculation of the AST is to convert the modal amount of apatite directly to a concentration of P_2O_5. The modes of apatite from each of the units and the amounts of P_2O_5 contributed from apatite (P_2O_5 = mode/2.06) are listed in table 5. The amount of P_2O_5 contributed from apatite is on the order of half of the whole-rock P_2O_5 which may be due to increasing $D^{AF/l}_{P_2O_5}$ and $D^{PL/l}_{P_2O_5}$ as crystallization proceeds as has been demonstrated by London, Loomis, and Huang (1990). The amount of P_2O_5 not in apatite is present in feldspars, micas, amphiboles, zircons, and other phosphates. When AST's are calculated using the P_2O_5 in apatite ($P_2O^*_5$ in table 5), they are generally 35°C lower than those calculated using the whole-rock P_2O_5. The AST's used in further calculations have been determined in this way, considering only the P_2O_5 in apatite (table 6).

TABLE 5

Data for the Tuolumne Intrusive Series

Unit	Whole Rock Chemistry				Mode
	SiO_2	P_2O_5	$P_2O^*_5$	$P_2O^r_5$	Apatite
Kuna Crest	58.7	.21	.11	.10	.22
Half Dome Equigranular	66.8	.16	.09	.06	.19
Half Dome Porphyry	67.8	.17	.10	.07	.20
Cathedral Peak	69.7	.14	.09	.05	.19
Johnson Porphyry	74.2	.03	.01	.02	.03

Analyses are from Bateman and others (1988). Abbreviations are as follows: Whole Rock: $P_2O^*_5$–amount of P_2O_5 that is present in the rock that is contained within the mineral apatite, expressed as g P_2O_5/100 g rock. These values are obtained by dividing the mode by 2.06 which is the conversion factor from mode apatite to g P_2O_5; $P_2O^r_5$ amount of residual P_2O_5, that is, P_2O_5 contained in mineral phases other than apatite.

TABLE 6

Calculated apatite saturation characteristics based on P_2O_5 in apatite

	Temperature	% Crystallization	$C^{l,AST}_{SiO_2}$	$C^{l,AST}_{P_2O_5}$
Kuna Crest	928	35	67.2	0.17
Half Dome Equigranular	901	9	69.8	0.10
Half Dome Porphyry	915	9	70.5	0.11
Cathedral Peak	925	9	72.3	0.10
Johnson Porphyry	795	16	74.7	0.02

Values in this table were calculated using the P_2O_5 in apatite only.

Given AST values, we can obtain estimates of the initial concentrations of the halogens in the melt and magmatic volatile phase using apatite compositions. Apatites were analyzed using the method described in app. 1 and are listed in table 7. Halogen concentrations in the magmatic volatile phase and the melt were calculated using eqs (18) and (19) for Cl and (23) and (24) for F.

Estimates of the concentrations of chlorine exhibit a regular pattern in the magmatic volatile phase and melt from rim to core in the TIS. Within the magmatic volatile phase, Cl was highest (27,000 ppm) within the KC, the unit that crystallized to yield the mafic rim of the TIS. Estimates of C^{aq}_{Cl} for the intermediate units, the HDE, HDP, and CP, range from 6100 to 19,000 ppm. The C^{aq}_{Cl} of the JP magma (the unit that makes up the core of the suite) was 3000 ppm. Within the KC, the concentration of Cl in the associated melt ($C^{l,AST}_{Cl}$) is estimated to have

TABLE 7

Composition of apatite from the Tuolumne Intrusive Suite

	KC	HDE	HDP	CP	JP
CaO	54.5	54.2	54.5	54.4	53.3
FeO	0.30	0.10	0.12	0.11	0.15
MgO	0.03	0.08	0.01	0.00	0.01
MnO	0.03	0.05	0.12	0.13	0.28
P_2O_5	40.7	42.0	40.6	40.4	41.0
SiO_2	0.12	0.13	0.23	0.14	0.11
Al_2O_3	0.06	0.08	0.06	0.06	0.04
Cl	0.20	0.08	0.04	0.03	0.01
F	2.29	3.05	2.47	3.12	3.34
OH(c)	0.65	0.32	0.60	0.30	0.20
Total	99.40	99.37	99.27	98.98	98.69
X^{Ap}_{ClAp}	0.030	0.006	0.006	0.005	0.002
X^{Ap}_{FAp}	0.61	0.81	0.66	0.83	0.89
X^{Ap}_{HAp}	0.36	0.18	0.34	0.17	0.11

Apatites contained within, or in contact exclusively with, anhydrous phases are included in this table. Complete list of analyses can be found in Piccoli (ms). Abbreviations are listed in table 4. These apatites have been analyzed using the method in app. 1. OH(c) has been calculated using the equation wt percent OH = 1.79 (1 − (wt percent F/3.767) − (wt percent Cl/6.809)) which assumes that apatite is stoichiometric in the halogen site.

been 620 ppm. Estimates of $C_{Cl}^{l,AST}$ for the intermediate units are 140 to 440 ppm. The JP (in the core of the suite) is estimated to have contained 69 ppm when the melt began to crystallize apatite. Trends of the estimates of F concentrations in the TIS are not as clear. Estimates of $C_F^{aq,AST}$ and $C_F^{l,AST}$ range from 46 to 130 ppm and 150 to 650 ppm, respectively (table 8).

In the general case, crystallization of phases during the cooling of a subliquidus, supersolidus, multicomponent system occurs over a range of temperatures except in the case of crystallization at a minimum or eutectic point. Magmatic apatite is no exception. On the other hand, thermodynamic calculations of fugacities and other composition-related variables are performed at a given temperature. To use the AST as the temperature of the calculation, we need to demonstrate that most of the apatite crystallizes over a rather restricted temperature interval (ΔT).

The quantity of apatite that crystallizes over a temperature interval can easily be calculated using a modified version of eq (1) (solved for $C_{P_2O_5}^{l}$ and converted to volume of apatite). This calculation has been performed for the plutons of the TIS, and the volume of apatite that crystallized over a given temperature interval is summarized in figure 4. The AST of each of the units can be read along the x-axis. The solidus has been modelled as being 680°C for each of the units. This analysis shows that over half the apatite in the granodioritic units crystallized within

TABLE 8

Calculated magmatic volatile phase and melt compositions

	KC	HDE	HDP	CP	JP
C_{Cl}^{aq}	27,000	19,000	6,000	10,000	3,000
$C_{Cl}^{l,AST}$	620	440	140	230	69
$C_{Cl}^{l,o}$	400	400	130	210	58
C_F^{aq}	46	98	66	130	61
$C_F^{l,AST(1)}$	230	480	320	650	290
$C_F^{l,o(1)}$	150	430	290	590	240
$C_F^{l,AST(2)}$	150	350	230	440	340
$C_F^{l,o(2)}$	100	320	210	400	290
$C_{Cl}^{l}/C_{H_2O}^{l}$	0.01	0.01	0.003	0.005	0.001
$C_F^{l}/C_{H_2O}^{l}$	0.003	0.009	0.006	0.01	0.007

All concentrations are in ppm. The AST's used in these calculation are listed in table 7. Values for C_{Cl}^{l} were calculated using the $D_{Cl}^{aq/l}$ described in the text. Values for C_F^{l} were calculated using the $D_F^{aq/l}$ from (1) Dingwell and Scarfe (1983) and (2) estimated from the data of table 3 of Webster and Holloway (1990) for water saturated melts with less than 10,000 ppm F at 2 kb. The apatite analyses used in the calculation are listed in table 7. $C_{Cl}^{l,o}$ and $C_F^{l,o}$ are calculated from $Cl_{Cl}^{l,AST}$ and $Cl_F^{l,AST}$ assuming crystal/melt incompatibility of the halogens prior to the crystallization of apatite and the crystallinities listed in table 6.

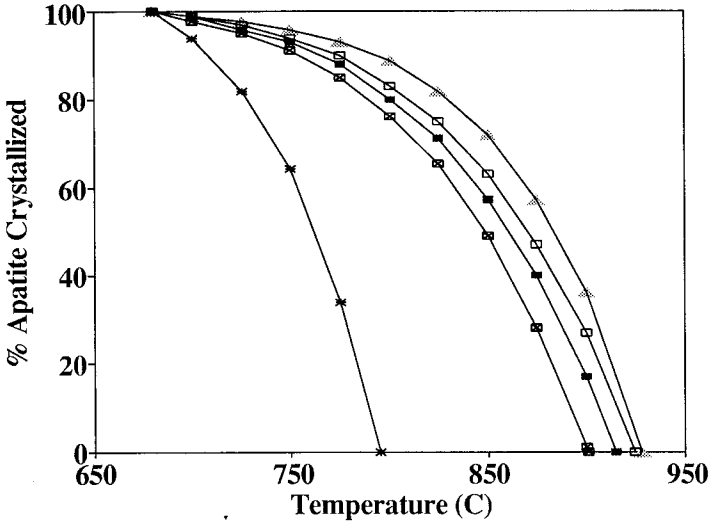

Fig. 4. Plot of the volume percent of apatite that crystallizes for each of the units in the Tuolumne Intrusive Series for a given cooling interval. The AST for each of the units can be read along the x-axis at 0 percent apatite crystallized. Symbols: triangle, Kuna Crest; open square with X, Half Dome Equigranular; filled square, Half Dome Porphyry; open square, Cathedral Peak; asterisk, Johnson Porphyry.

60°C of their respective AST's. Further, within the JP, half of the apatite crystallized within 30°C of the AST. From the initiation of crystallization of apatite, the temperature-rate at which apatite grows decreases (dV_{ap}/dT) monotonically as the solidus is approached. Although it is meaningless to discuss a unique temperature at which a single grain of apatite crystallizes, the majority of apatite in a rock crystallizes within a small ΔT of the AST. It is important to note, however, that within each of the units of the TIS, there is some variation in SiO_2 and P_2O_5 and therefore variation in model AST's.

Discussion

Within the TIS, the highest estimates of $C_{Cl}^{l,AST}$ are in the KC (620 ppm) and HDE (440 ppm) (table 8). Although the estimates of $C_{Cl}^{l,AST}$ differ by 180 ppm, the calculations suggest nearly equal values for $C_{Cl}^{l,o}$ (400 ppm). The halogens in these calculations have been treated as having incompatible behavior prior to apatite crystallization. The initial value of 400 ppm Cl in the KC and HDE increased by different amounts at apatite saturation in these two units, because of the variation in AST. The KC is estimated to have crystallized 35 percent prior to saturation with apatite, whereas the HDE crystallized only 9 percent. The remainder of the units have been estimated to have had chlorine concentrations at the AST ($C_{Cl}^{l,AST}$) between 58 and 210 ppm.

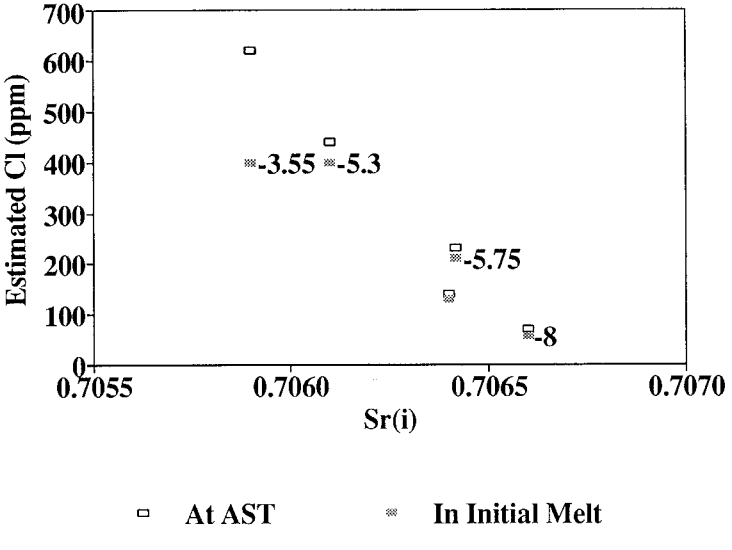

Fig. 5. Plot of the estimated initial Cl concentration using apatite chemistry versus $(^{87}Sr/^{86}Sr)_i$ for the rocks of the Tuolumne Intrusive Suite. The $(^{87}Sr/^{86}Sr)_i$ represent the averages of each of the units from a traverse through the western portion of the suite. In parentheses are $\epsilon_{Nd}(T)$ for the respective units ($\epsilon_{Nd}(T)$ data do not exist for the Half Dome Porphyry). The isotopic data are from Kistler and others (1986).

The results for F in the aqueous phase and the melt are not as clear. Examination of tables 7 and 8 reveals an interesting relationship between estimated C_F^{aq}, halogen content of apatites, and host rock chemistries. Estimates of C_F^{aq} are lowest in the KC (46 ppm) and JP (61 ppm), the most mafic and most felsic units in the TIS, whereas the remainder of the units contain higher values (66-130). This appears somewhat perplexing: $X_{FAp}^{Ap}/X_{HAp}^{Ap}$ in the KC is the lowest of any of the units (1.7) whereas those in the JP are the highest (8.0). Additionally, the $X_{ClAp}^{Ap}/X_{HAp}^{Ap}$ is highest in the KC (0.08), which yields the highest estimates of Cl, and this has a significant effect on the estimated F concentrations. Conversely, the $X_{ClAp}^{Ap}/X_{HAp}^{Ap}$ is lowest in the JP (0.02). Upon examination of eq (23), the most important factors in estimating C_F^{aq} are $X_{FAp}^{Ap}/X_{HAp}^{Ap}$, pressure, and temperature. The JP, with the highest $X_{FAp}^{Ap}/X_{HAp}^{Ap}$, is estimated to have the lowest C_F^{aq} (61 ppm). The reason for this is that the AST for the JP (795°C) is 133°C lower than the KC (928°C).

Chlorine in the melt and the magmatic volatile phase exhibit a relatively smooth trend across the TIS. Kistler and others (1986), in a detailed isotopic study, reported both strontium and neodymium isotope systematics within the TIS (the data are summarized in table 4). The units with the lowest $(^{87}Sr/^{86}Sr)_i$, the KC (0.7059), and HDE (0.7061) have the highest estimated $C_{Cl}^{l,AST}$ and $C_{Cl}^{l,o}$ within the suite. Furthermore, the JP has the highest $(^{87}Sr/^{86}Sr)_i$ (0.7066) and the lowest estimated $C_{Cl}^{l,AST}$ and $C_{Cl}^{l,o}$.

The opposite relation can be seen between $\epsilon_{Nd}(T)$ and Cl. The KC has the lowest $\epsilon_{Nd}(T)$ (−3.5), whereas the JP has the highest (−8.0). In light of these isotopic systematics, it may be suggested that chlorine has been incorporated into the source regions of the more (isotopically) primitive component of the TIS. The Cl in the system may have been added to the source region by a subduction-related component. This is consistent with the findings of Ishihara and Sasaki (1989) who imply that variations in $\delta^{34}S$ in the granites of the central Sierra Nevada batholith reflect variations in the proportions of a subduction-related component.

Unlike the Bishop Tuff example, a significant amount of crystallization has taken place prior to the initiation of apatite crystallization, ranging from 9 to 35 percent (table 6). During this time, the concentration of Cl and F are building up in the melt. However, if a melt becomes saturated with a volatile phase, the Cl content in that melt may not build up (Candela, 1986). The initial halogen concentrations in the melt ($C_{Cl}^{l,o}$ and $C_F^{l,o}$) have been calculated using $C_{Cl}^{l,AST}$ and $C_F^{l,AST}$ and estimates of the crystallinity of the magma (for each of the respective units) at the AST assuming incompatibility of the halogens in the melt. The "backcalculated" melt values range from 58 to 400 ppm Cl and 100 to 430 ppm F, which are estimates of initial Cl and F.

DISCUSSION OF UNCERTAINTY IN CALCULATIONS

The model calculation described here defines, for the first time, a method of estimating the initial halogen content of felsic magmas for a given initial water content. Standard error propagation techniques (Mandel, 1964) have been employed so that estimates of uncertainty could be made for this calculation. Due to the nature of the equations used to estimate $C_{Cl}^{l,AST}$, $C_{Cl}^{l,o}$, $C_F^{l,AST}$, and $C_F^{l,o}$, uncertainty must be considered as a function of the uncertainties in the variables $X_{ClAp}^{Ap}/X_{HAp}^{Ap}$, $X_{FAp}^{Ap}/X_{HAp}^{Ap}$, $D_{Cl}^{aq/l}$, $D_F^{aq/l}$, $\log_{10}(HCL/\Sigma Cl)^{aq}$, and equilibrium constants. Each of these sources of uncertainty will be considered below.

Due to the large number of variables involved in these estimates, it is not practical to calculate an uncertainty that is valid for all conditions. Here, the propagation of uncertainty is demonstrated for apatites from the Kuna Crest pluton of the Tuolumne Intrusive Suite.

Equilibrium Constant

Obtaining an estimate of the uncertainty on calculated equilibrium constants is sometimes difficult. Two methods can be used to obtain an estimate of the uncertainty of eqs (9) and (22) from either the raw thermodynamic data ($\Delta\overline{G}_{rxn}$; converted to an equilibrium constant) or directly from the equilibrium constant. Zhu and Sverjensky (1991), the source of data from the apatite endmembers used in this study, do not report the uncertainty associated with $\Delta\overline{G}_f^o$ for ClAP, FAp, and HAp; however, they report uncertainty in the form of equilibrium constants for statements of equilibrium that are the same as those stated in eqs (4) and (20). They report the uncertainty associated with the statement of equilib-

rium in eq (4) as 0.16 (2σ log K: 2 kb values have been averaged here) which leads to a coefficient of variation (CV) of 0.0396 (given the value of the equilibrium constant calculated using eq (9)) for conditions of apatite saturation in the granodioritic to quartz-dioritic Kuna Crest. Similarly, for the statement of equilibrium described in eq (22), Zhu and Sverjensky report an uncertainty of 0.195 (2σ log K) which leads to a CV of 0.0243. The higher uncertainty associated with statements of equilibrium which contain Cl species reflects the greater uncertainty of the fundamental thermodynamic properties associated with Cl species as discussed by Tacker and Stormer (1989).

Uncertainty Associated with Apatite Composition

As stated above, apatites from the Kuna Crest have arbitrarily been used in making estimates of the uncertainty within the model. The composition of apatites from the Kuna Crest are reported in table 7 and are as follows: $X^{Ap}_{ClAp} = 0.03$, $X^{Ap}_{FAp} = 0.61$, and $X^{Ap}_{HAp} = 0.36$. These lead to values for $X^{Ap}_{ClAp}/X^{Ap}_{HAp}$ of 0.08 and $X^{Ap}_{FAp}/X^{Ap}_{HAp}$ of 1.7. The uncertainty of these values based on counting statistics are reported in the discussion of apatite analyses in app. 1.

Uncertainty in log $HCL/\Sigma Cl^{aq}$

A large source of uncertainty in the model calculations is due to the relationship between HCl and total chloride in the aqueous phase. These data, reviewed in eq (16), inherently have considerable scatter due to the nature of the experiments. For the 2.2 kb experimental runs of Shinohara (ms) the average $\log_{10}(HCl/\Sigma Cl)^{aq} = -1.30$. The average standard estimate of error of $\log_{10}(HCl/\Sigma Cl)^{aq}$ over the pressure range of Shinohara's experiments (0.6-6.7 kb) as described by eq (16) is 0.31 log units (theoretically this value should become smaller at low pressures and larger at higher pressures). Shinohara (ms) suggests that the considerable spread in the Cl speciation data in the MVP is due to variable amounts of HCl loss during his washing and distillation procedure. The CV associated with the relationship between HCl and total Cl is 0.2366.

Uncertainty in D

Uncertainty associated with two MVP/melt partition coefficients must be considered: $D^{aq/l}_{Cl}$ and $D^{aq/l}_{F}$. The data used to formulate $D^{aq/l}_{Cl}$ and $D^{aq/l}_{F}$ are reviewed in eqs (25) and (26). For the 2.2 kb runs of Shinohara (ms) the average $D^{aq/l}_{Cl}$ is 60.7, with a 1σ uncertainty of ± 17. This corresponds to a CV of 0.280.

The uncertainty associated with $D^{aq/l}_{F}$ is much smaller. Assuming a temperature of 900°C (which is an appropriate temperature as suggested in the examples that follow), $D^{aq/l}_{F} = 0.28$ with an uncertainty of ± 0.028. This corresponds to a CV of 0.1.

Overall Uncertainty

Given the uncertainties described above, the overall uncertainty in calculating initial halogen concentrations can be calculated. When a function is written in terms of purely multiplicative form (as are the equations for $C_{Cl}^{l,AST}$, $C_{Cl}^{l,o}$, $C_{F}^{l,AST}$, and $C_{F}^{l,o}$) the law of propagation of errors takes a simple additive form when components are written in terms of relative error (for example, coefficients of variation) (Mandel, 1964) assuming that the error takes the form of a Gaussian function (which may or may not be the case here) and that the error of the individual components is not correlated. For example, from eq (19), the following can be derived,

$$(CV_{apt\ Cl}) = \sqrt{(CV_{apt\ analyses})^2 + (CV_{K_{aq}})^2 + (CV_{D_{Cl}^{aq/l}})^2 + (CV_{HCl/\Sigma Cl^{aq}})^2} \quad (27)$$

which was used for obtaining values in the following discussion. It is important to note that the estimated uncertainty is valid only at the conditions described above (that is, at 900°C, for $X_{ClAp}^{Ap}/X_{HAp}^{Ap} = 0.08$ and $X_{FAp}^{Ap}/X_{HAp}^{Ap} = 1.7$, et cetera) for apatites from the Kuna Crest. It is therefore more useful to express these in terms of CV which can then be converted to absolute amounts. Given these conditions, the following values were obtained (1σ): $C_{Cl}^{aq} = 27{,}000 \pm 6900$ (CV = 0.255), $C_{Cl}^{l,o} = 400 \pm 150$ (CV = 0.379), $C_{F}^{aq} = 46 \pm 4$ (CV = 0.092), and $C_{F}^{l,o} = 125 \pm 17$ (CV = 0.136).

As can be seen from these calculated values, the uncertainty associated with Cl species are greater than those for F. This is true for two reasons: greater uncertainty associated with the thermodynamic properties of ClAp and uncertainty in determining the relationship between HCl and total Cl in the aqueous phase (all F in the aqueous phase is present as HF).

Although this uncertainty appears rather large (from 10-40 percent) it is dependent almost entirely upon the uncertainty in $\Delta\overline{G}_f^o$ of apatite endmembers and determining the relationship between HCl and total Cl in the MVP. Experiments are currently being performed that may yield greater accuracy of these apatite endmember thermodynamic properties (R.C. Tacker, personal communication) and Cl speciation (T.J. Williams, personal communication). The model can be easily modified as this information becomes available. Application of this technique to the PBT suggests that the true error may in fact be much less than that given by the error propagation equation.

Discussion

The concentration of halogens in felsic magmas has important implications for the modeling of magmatic properties and processes, including magma rheology (viscosity and diffusion) and ore deposit petrogenesis. Dingwell (1987) has shown that increasing amounts of F in rhyolitic melts has an effect of decreasing viscosity, which in turn increases the probability that a magma will migrate and erupt at the

surface. Dingwell (1987), Watson (1991), and Baker and Watson (1988) have shown that the diffusion rate of many cations in felsic magmas are increased in the presence of increased Cl and F abundances in the melt. Candela (1989a,b) has performed calculations in which he suggests that the initial Cl/H_2O in melts is important in determining the efficiency with which a magmatic fluid can concentrate an ore metal (for example, copper) and transport it to the site of deposition.

Application of eq (16) relating HCl to total Cl in the aqueous phase represents a crucial step in this model. Examination of eq (15) demonstrates the influence of the aluminum saturation index (ASI) of the melt on $(HCl/\Sigma Cl)^{aq}$ in the magmatic volatile phase. Additionally, inspection of eq (15) suggests that $(HCl/\Sigma Cl)^{aq}$ is also dependent upon the activity of SiO_2 in the melt ($a^{l}_{SiO_2}$). At the apatite saturation temperature, the greater deviation of the $a^{l}_{SiO_2}$ from quartz saturation, the lower the ratio of $(HCl/\Sigma Cl)^{aq}$ in eq (15). The melt compositions in the experiments of Shinohara (ms) and Shinohara, Iiyama, and Matsuo (1984) which were used to derive this equation are close to saturation with quartz under the conditions in which the experiments were performed. An $a^{l}_{SiO_2}$ less than $a^{l,QSAT}_{SiO_2}$ implies that estimates of C^{aq}_{Cl} and $C^{l,o}_{Cl}$ should be increased due to the underestimation of $(HCl/\Sigma Cl)^{aq}$. This is an important consideration for melts with low $C^{l}_{SiO_2}$; however, this has little effect on the more silicic systems.

This is an important consideration when interpreting results from more mafic (granodioritic to quartz-dioritic) rocks. Adjustments can be made to estimates of initial halogen concentrations and magmatic volatile phase composition if estimates of $C^{l,AST}_{SiO_2}$ can be made. Unfortunately, experimental data of this type do not exist for silicic melts. However, Nekvasil (1988a,b) and Burnham and Nekvasil (1986) present a model that can be used to calculate $a^{l}_{SiO_2}$ for a variety of initial, silicic melt compositions. This model was used to calculate the activity of SiO_2 at the AST relative to that at quartz saturation ($a^{l,AST}_{SiO_2}/a^{l,QSAT}_{SiO_2}$). This ratio can then be used as an index of the degree of quartz saturation, and estimates of halogen concentrations of melts can therefore be the temperatures of interest, the AST and the quartz saturation temperature, the $a^{l}_{SiO_2}$ and $a^{l,QSAT}_{SiO_2}$ were calculated using the activity composition relationships in table 2C and eq (1), respectively, of Burnham and Nekvasil (1986). This exercise was completed for the PBT and the various formations of the TIS. The ($a^{l,AST}_{SiO_2}/a^{l,QSAT}_{SiO_2}$) in the PBT is nearly one, as the melt is nearly quartz saturated at the AST, and no corrections need to be made to $C^{l,AST}_{Cl}$. As expected, in the KC, the ratio of $a^{l,AST}_{SiO_2}$ to $a^{l,QSAT}_{SiO_2}$ is not unity but is equal to approx 0.84, which suggests that the melt is below quartz saturation at the temperature of apatite saturation. Although this ratio is 0.84, it has the effect of raising the estimates of $C^{l,AST}_{Cl}$ by 40 percent

because $a^{l}_{SiO_2}$ is cubed in eq (15). Effectively, the $C^{l,AST}_{Cl}$ would be ~870 ppm and not 620 ppm. Within the remainder of the units of the TIS, the ratio $a^{l,AST}_{SiO_2}/a^{l,QSAT}_{SiO_2}$ range from 0.94 to 1, which leads to the remainder of the estimates of $C^{l,AST}_{Cl}$ being too low by at most 17 percent.

The "model" calculation described here has been defined to calculate initial halogen content of felsic magmas for a given initial water content something that previously could not be done. Based on the comparison of estimated initial halogen concentrations with Bishop Tuff melt inclusion data, the application of this technique suggests that the true error may in fact be much less than that given by the error propagation equation (estimated to be 10-40 percent).

The estimation of the initial water content of the melts of interest is very important when utilizing this model, as erroneous estimates of initial water lead to error in estimated liquidus temperatures and erroneous crystallinity at the AST and a systematic error in the use of eq (16). The presence of amphibole at most locations within the TIS and an estimate of intrusion pressure (2 kb) confines the initial water content to 4 to 6 wt percent (that is, the initial water content cannot vary significantly). Within the PBT, measured water contents of melt inclusions suggest 5.7 wt percent H_2O at the time of crystallization. If an appropriate estimate of initial magmatic water concentrations can be made, our technique is useful in estimating initial halogen concentrations. Our technique could, however, easily be modified for melts with different estimates of initial water. This method can yield considerably more accurate and precise information as more temperature-melt composition and temperature-crystallinity information is obtained in the future.

CONCLUSIONS

Changes in the ratios $f^{aq}_{HCl}/f^{aq}_{H_2O}$ and $f^{aq}_{HF}/f^{aq}_{H_2O}$ have been inferred from halogen concentrations in apatite. Moreover, rather than assuming an arbitrary magmatic temperature, the temperature at which the apatite begins to crystallize has been estimated for a variety of natural granitic compositions given published apatite solubility data. These factors have been used in conjunction with estimates of melt composition at the time of apatite crystallization to yield estimates of initial Cl and F in the magmatic volatile phase and the "model" initial silicic melt.

Apatite within the plinian Bishop Tuff is estimated to have begun crystallizing at 860°C. This estimate has been used in combination with apatite analyses to generate estimates of magmatic volatile phase Cl and F concentrations of 31,000 to 42,000 ppm and 38 to 60 ppm, respectively. Given volatile phase/melt experimental data, these estimates suggest 700 to 960 ppm and 160 to 300 ppm Cl and F in the initial Bishop Tuff melt, respectively. These values compare favorably with measured Cl and F concentrations in melt inclusions.

The units of the Tuolumne Intrusive Suite are estimated to have crystallized between 9 to 35 percent before the apatite saturation tempera-

tures of 928° to 795°C were reached. Estimations of $C^{l}_{SiO_2}$ have been made for each of the units in the TIS. Analysis of apatite solubility function suggests that over half the apatite crystallizes in this system within 60°C of the AST. Estimates of initial melt Cl and F concentrations are 58 to 400 and 150 to 590 ppm, respectively. The inferred concentration of chlorine in the melt decreases from rim to core of the TIS and corresponds with an increase in $(^{87}Sr/^{86}Sr)_i$ and decrease in $\epsilon_{Nd}(T)$, suggesting that a variable amount of a subduction related component may control melt Cl in this zoned intrusive system.

ACKNOWLEDGMENTS

The comments of reviewers is greatly appreciated. Thanks are in order for Tom Williams and Steve Lynton and the rest of the members of the Laboratory for Mineral Deposits Research, whose discussions about apatite-melt-volatile phase equilibria were very helpful. Tom Williams's and Steve Lynton's reviews of the equations in this manuscript are also appreciated. We thank Hanna Nekvasil for providing the program PATH, which allowed us to calculate SiO_2 activities. Jay Ague's help in ascertaining the accuracy of our apatite analyses was insightful and is appreciated. Chen Zhu provided early drafts of manuscripts concerning various aspects of apatite equilibria, and they were also greatly appreciated. Eugene Jarosewich is thanked for providing microprobe standards from the Smithsonian Museum. We would like to acknowledge funding from the National Science Foundation (EAR-8706198 and EAR-9004154) and the Department of Energy (DOE-DEFG0790ID13025) to PAC and dissertation support from the University of Maryland as a Dissertation Fellowship, Sigma Xi, Geological Society of America, and the Gem, Lapidary, and Mineral Society of Montgomery County, Maryland, to PMP.

APPENDIX

Analysis of Apatites from the Tuolumne Intrusive Suite for Cl and F

Successful analysis of the halogens in apatite is essential in the utilization and interpretation of the model presented here. However, the analysis of apatites for halogens by electron probe microanalyzer is commonly problematic. Halogen analyses are difficult, especially $F_{K\alpha}$, for a variety of reasons: (1) major element peak overlaps, (2) mobility of the halogens under the electron beam, and (3) absorption of the halogens.

Critical to effective apatite analysis is the separation of the peaks $F_{K\alpha}$(1st order) and $P_{K\alpha(1,2)}$(3rd order). Although these are found in the same spectrometer position ($F(n\lambda) = 18.320$; $P(n\lambda) = 18.474$), they have drastically different energies ($F_{K\alpha} = 0.677$; $P_{K\alpha(1,2)} = 2.013$). These can easily be separated using a Single Channel Analyzer (SCA). The SCA allows for the separation of peaks at the same spectrometer position, if the peaks have different energies (for a discussion, see Goldstein and others, 1992). This effect is commonly overlooked in the literature and may result in F contents in apatite greater than 3.76 wt percent (more F than stoichiometric fluorapatite). The SCA has been utilized in obtaining the analyses listed in table 7. Calibration of the SCA window was determined for fluorine and phosphorus using fluorite and hydroxyapatite, respectively, in order to maximize count rates and simultaneously avoid overlap problems.

Diffusion of the halogens is also a significant problem when analyzing apatites (Potts, 1987; Goldstein and others, 1992). Diffusion of light elements appears to be caused by thermal decomposition of minerals (Potts, 1987), although the exact mechanism appears to be complex. Diffusion of the halogens has been reduced in these analyses by (1) increasing the beam size so that the beam intensity is reduced, (2) rastering the beam so that the sample has a chance to cool as the beam is moving, and (3) analyzing F and Cl first (simultaneously) so that the apatite has less time to decompose. Ideally, a cooling stage would be used to reduce this effect further. Time diffusion studies, similar to those of Stormer, Pierson, and Tacker (1991), were performed on oriented Durango Apatite mounts, and it was determined in our study that diffusion was not significant using the operating conditions described here.

The low energy of the $F_{K\alpha}$ x-ray (0.677 KeV) allows for a large amount of absorption to occur under standard microanalysis conditions (15 kV). This overvoltage ($15/0.677 \sim 22$) is approximately twice the maximum idealized value (3-10) recommended for microanalysis. This leads to low count rates for F. This effect is not nearly as drastic for Cl whose energy is 2.621 KeV. Two steps can be taken to reduce this effect: (1) count for extended periods of time to increase counting statistics, and (2) reduce the accelerating voltage so that absorption of $F_{K\alpha}$ X-rays is not as prevalent (however, this does not allow for the analysis of many of the higher energy X-rays). Further, as was demonstrated by Kerrick, Eminhizer, and Villaume (1973), significant absorption of $F_{K\alpha}$ X-rays may also occur due variation in thickness of carbon coat between standards and unknowns. This problem was alleviated by coating standards and unknowns simultaneously.

The apatites from the Tuolumne Instrusive Suite were analyzed at the Central Facility for Microanalysis at the University of Maryland. They were analyzed using a JEOL 840 electron probe microanalyzer with a Tracor Northern 5500 Series II operating system. A variety of beam widths and cup currents were tested for diffusion and volatilization, and it was found that a rastered beam of 10×10 μm, at a cup current of 10 nA, and an accelerating voltage of 15 KeV, was optimal. Count times for the halogens averaged 120 sec. Cl and F were analyzed using PET and TAP crystals, respectively. Apatites were checked for zoning with respect to the halogens, and it was found not to be present. Major elements were analyzed simultaneously. Durango Apatite (USNM 104021) was used as a standard for Ca, P, F, and Cl (54.02 percent CaO, 40.78 percent P_2O_5, 3.53 percent F, 0.41 percent Cl). The standard deviation (1σ) due to counting statistics only are as follows: Ca < 1.00 percent, P < 1.00 percent, F ~4 percent (Kuna Crest), Cl ~4 percent (Kuna Crest), F ~3 percent (Johnson Porphyry) and Cl ~6 percent (Johnson Porphyry).

The averages of the apatites from each of the units in the TIS are listed in table 7. These apatites are included within or associated with anhydrous phases only. The apatites recorded in this table represent average analyses from each of the units of the TIS, most of which exhibit some compositional variation within each unit. The variability in apatite composition (in mole fraction) can be expressed as follows (1σ): Kuna Crest—$X^{Ap}_{ClAp} = 0.030 \pm 0.004$, $X^{Ap}_{FAp} = 0.61 \pm 0.004$; and for the Johnson Porphyry—$X^{Ap}_{ClAp} = 0.002 \pm 0.002$, $X^{Ap}_{FAp} = 0.89 \pm 0.050$. Some of this variability is undoubtedly due to intra-unit variations; however, these are beyond the scope of this study.

References

Ague, J. J., and Brimhall, G. H., 1988a, Regional variations in bulk chemistry, mineralogy, and the compositions of mafic and accessory minerals in the batholiths of California: Geological Society of America Bulletin, v. 100, p. 891–911.

———— 1988b, Magmatic arc symmetry and distribution of anomalous plutonic belts in the batholiths of California: effects of assimilation, crustal thickness, and depth of crystallization: Geological Society of America Bulletin, v. 100, p. 912–927.

Anderson, A. T., Jr., Newman, S., Williams, S. N., Druitt, T. H., Skirius, C., and Stolper, E., 1989, H2O, CO2, Cl, and gas in Plinian and ash-flow Bishop rhyolite: Geology, v. 17, p. 221–225.

Anderson, A. T., Jr., Skirius, C., Williams, S. N., Druitt, T., Newman, S., and Stolper, E., 1988, H2O, CO2, Cl and gas in the Bishop rhyolite: EOS (Transactions of the American Geophysical Union), v. 69, p. 529.

Baker, D. R., and Watson, E. B., 1988, Diffusion of major and trace elements in compositionally complex Cl- and F-bearing silicate melts: Journal of Non-Crystalline Solids, v. 102, p. 62–70.

Barbarin, B., 1991, Enclaves of the Mesozoic calc-alkaline granitoids of the Sierra Nevada batholith, California, *in* Didier, J., and Barbarin, B., editors, Enclaves and Granite Petrology: New York, Elsevier, p. 135–153.

Bateman, P. C., 1988, Constitution and genesis of the central part of the Sierra Nevada Batholith, California: United States Geological Survey Open File Report 88–382.

Bateman, P. B., and Chappell, B. W., 1979, Crystallization, fractionation, and solidification of the Tuolumne Intrusive Series, Yosemite National Park, California: Geological Society of America Bulletin, v. 90, p. 465–482.

Bateman, P. C., Chappell, B. W., Kistler, R. W., Peck, D. L., and Busacca, A., 1988, Tuolumne Meadows Quadrangle, California-analytic data: United States Geological Survey Bulletin 1819, 43 p.

Bergantz, G., 1990, Melt fraction diagrams: The link between chemical and transport models, *in* Nicholls, J., and Russell, J. K., editors, Modern Methods of Igneous Petrology: Understanding Magmatic Processes: Reviews in Mineralogy, v. 24, p. 239–257.

Boudreau, A. E. and Kruger, F. J., 1990, Variation in the composition of apatite through the Merensky Cyclic Unit in the western Bushveld Complex: Economic Geology, v. 85, p. 737–747.

Boudreau, A. E., and McCallum, I. S., 1989, Investigations of the Stillwater Complex: Part V. Apatites as indicators of evolving fluid composition: Contributions to Mineralogy and Petrology, v. 102, p. 138–153.

Boudreau, A. E., Mathez, E. A., and McCallum, I. S., 1986, Halogen geochemistry of the Stillwater and Bushveld complexes: Evidence for transport of platinum group elements by Cl-rich fluids: Journal of Petrology, v. 27, p. 967–986.

Burnham, C. W., and Nekvasil H., 1986, Equilibrium properties of granite pegmatite magmas: American Mineralogist, v. 71, p. 239–263.

Candela, P. A., 1986, Towards a thermodynamic model for the halogens in magmatic systems; An application to melt-vapor-apatite equilibria: Chemical Geology, v. 57, p. 289–301.

———— 1989a, Magmatic ore-forming fluids: Thermodynamic and mass transfer calculations of metal concentrations, *in* Whitney, J. A., and Naldrett, A. J., editors, Ore Deposits Associated with Magmas: Reviews in Economic Geology, v. 4, p. 203–221.

———— 1989b, Felsic magmas, volatiles, and metallogenesis, *in* Whitney, J. A., and Naldrett, A. J., editors, Ore Deposits Associated with Magmas: Reviews in Economic Geology, v. 4, p. 223–233.

———— 1990, Theoretical constraints on the chemistry of the magmatic aqueous phase, *in* Stein, H. J., and Hannah, J. L., editors, Ore-bearing Granite Systems; Petrogenesis and mineralizing processes: Geological Society of America Special Paper 246, p. 11–20.

Chappell, B. W. and White, A. J. R., 1991, Restite enclaves and the restite model, *in* Didier, J., and Barbarin, B., editors, Enclaves and Granite Petrology: New York, Elsevier, p. 375–381.

Clemens, J. D., Holloway, J. R., and White, A. J. R., 1986, Origin of A-type granite: Experimental constraints: American Mineralogist, v. 71, p. 317–324.

Creaser, R. A., and Gray, C. M., 1992, Preserved initial $^{87}Sr/^{86}Sr$ in apatite from altered felsic igneous rocks: A case study from the Middle Proterozoic of South Australia: Geochimica et Cosmochimica Acta, v. 56, p. 2789–2795.

Crisp, J. A., and Spera, F. J., 1987, Pyroclastic flows and lavas of the Mogan and Fataga Formations, Tejeda Volcano, Gran Canaria, Canary Islands: Mineral chemistry, intensive parameters, and magma chamber evolution: Contributions to Mineralogy and Petrology, v. 96, p. 503–518.

Dilles, J. H., 1987, Petrology of the Yerington Batholith, Nevada: Evidence for evolution of porphyry copper ore fluids: Economic Geology, v. 82, p. 1750–1789.

Dingwell, D. B., 1987, The structures and properties of fluorine rich magmas: a review of experimental studies, *in* Taylor, R. P., and Strong, D. F., editors, Recent Advances in the Geology of Granite-Related Mineral Deposits: Canadian Institute of Mining and Metallurgy Special Volume 39, p. 1–12.

Dingwell, D. B., and Scarfe, C. M., 1983, Major element partitioning in the system haplogranite-HF-H2O: implications for leucogranites and high-silica rhyolites: EOS (Transactions of the American Geophysical Union), v. 64, p. 342.

Dunbar, N. M., and Hervig, R. L., 1990a, Volatile gradient within the upper portion of the Bishop magma chamber: Evidence from ion microprobe analyses of melt inclusions: EOS (Transactions of the American Geophysical Union), v. 71, p. 651.

———— 1990b, Water, fluorine, and chlorine in the upper levels of silicic magma chambers: Implications for the presence of fluids in magmas: Goldschmidt Conference Abstracts, v. 2, p. 43.

Dunbar, N. M., and Hervig, R. L., 1992, Petrogenesis and volatile stratigraphy of the Bishop Tuff: Evidence from melt inclusion analysis: Journal of Geophysical Research, v. 92, p. 15129.

Egan, E. P., Wakefield, Z. T., and Elmore, K. L., 1950, High-temperature heat content of hydroxyapatite: American Chemical Society Journal, v. 72, p. 2418–2421.

Ekstrom, T. K., 1973, The distribution of fluorine among some coexisting minerals: Contributions to Mineralogy and Petrology, v. 34, p. 192–200.

Elliott, J. C., and Young, R. A., 1973, Conversion of single crystals of chlorapatite into single crystals of hydroxyapatite: Nature, v. 214, p. 904–906.

Gardner, J. E., Sigurdsson, H., and Carey, S. N., 1991, Eruption dynamics and magma withdrawal during plinian phase of the Bishop Tuff eruption, Long Valley Caldera: Journal of Geophysical Research, v. 96, p. 8097–8111.

George, W. O., 1924, The relation of the physical properties of natural glasses to their chemical composition: Journal of Geology, v. 32, p. 353–371.

Ghiorso, M. S., 1987, Modeling magmatic systems: thermodynamic relations, *in* Nicholls, J., and Russell, J. K., editors, Modern Methods of Igneous Petrology: Understanding Magmatic Processes: Reviews in Mineralogy, v. 24, p. 443–465.

Ghiorso, M. S., and Carmichael, I. S. E., 1987, Modeling magmatic systems: petrologic applications, *in* Nicholls, J., and Russell, J. K., editors, Modern Methods of Igneous Petrology: Understanding Magmatic Processes: Reviews in Mineralogy, v. 24, p. 467–469.

Gill, J. B., 1981, Orogenic Andesites and Plate Tectonics: New York, Springer-Verlag, 390 p.

Goldstein, J. I., Newbury, D. E., Echlin, P., Joy, D. C., Romig, A. D., Jr., Lyman, C. E., Fiori, C., and Lifshin, E., 1992, Scanning Electron Microscopy and X-ray Microanalysis: A Text for Biologists, Material Scientists, and Geologists: New York, Plenum Press, 820 p.

Green, T. H., and Watson, E. B., 1982, Crystallization of apatite in natural magmas under high pressure, hydrous conditions, with particular reference to 'Orogenic' rock series: Contributions to Mineralogy and Petrology, v. 79, p. 96–102.

Gunow, A. J., *ms*, 1983, Trace element mineralogy in the porphyry molybdenum environment: Ph.D. thesis, University of Colorado.

Hammarstom, J. M., and Zen, E-an, 1986, Al in hornblende: an empirical igneous geobarometer: American Mineralogist, v. 71, p. 1297–1313.

Harrison, T. M., and Watson, E. W., 1984, The behavior of apatite during crustal anatexis: Equilibrium and kinetic considerations: Geochimica et Cosmochimica Acta, v. 48, p. 1467–1477.

Helz, R. T., 1976, Phase relations of basalts in their melting range at PH2O = 5kb. Part II. Melt compositions: Journal of Petrology, v. 17, p. 139–193.

Heming, R. F., and Carmichael, I. S. E., 1973, High-temperature pumice flows from the Rabaul Caldera Papua, New Guinea: Contributions to Mineralogy and Petrology, v. 38, p. 1–20.

Hildreth, E. W., *ms*, 1977, The magma chamber of the Bishop Tuff: gradients in temperature, pressure, and composition: Ph.D. thesis, University of California-Berkeley, 328 p.

———— 1979, The Bishop Tuff: Evidence for the origin of compositional zonation in silicic magma chambers, *in* Chapin, C. E., and Elston, W. E., editors, Ash Flow Tuffs: Geological Society of America Special Paper 180, p. 43–75.

———— 1981, Gradients in silicic magma chambers: implications for lithospheric magmatism: Journal of Geophysical Research, v. 86, p. 10153–10192.

Hildreth, W., and Moorbath, S., 1988, Crustal contributions to arc magmatism in the Andes of Central Chile: Contributions to Mineralogy and Petrology, v. 98, p. 455–489.

Ishihara, S., and Sasaki, A., 1989, Sulfur isotopic ratios of the magnetite-series and ilmenite-series granitoids of the Sierra Nevada batholith—A reconnaissance study: Geology, v. 17, p. 788–791.

Johnson, M. C., and Rutherford, M. J., 1989, Experimentally determined conditions in the Fish Canyon Tuff, Colorado, magma chamber: Journal of Petrology, v. 30, p. 711–737.

Juster, T. C., Grove, T. L., and Perfit, M. R., 1989, Experimental constraints on the generation of FeTi basalts, andesites, and rhyodacites at the Galapagos Spreading Center, 85 W and 95 W: Journal of Geophysical Research, v. 94, p. 9251–9274.

Kerrick, D. M., Eminhizer, L. B., and Villaume, J. F., 1973, The role of carbon film thickness in electron microprobe analysis: American Mineralogist, v. 58, p. 920–925.

Kesler, S. E., Issigonis, M. J., Brownlow, A. H., Damon, P. E., Moore, W. J., Northcote, K. E., and Preto, V. A., 1975, Geochemistry of biotites from mineralized and barren intrusive systems: Economic Geology, v. 70, p. 559–567.

Kistler, R. W., Chappell, B. W., Peck, D. L., and Bateman, P. C., 1986, Isotopic variations in the Tuolumne Intrusive Series, California: Contributions to Mineralogy and Petrology, v. 94, p. 205–220.

Kogarko, L. N., and Romanchev, B. P., 1990, Apatite crystallization temperatures at the Kirunavara Deposit: Geokhimiya, no. 2, p. 237–243.

Kontak, D. J., and Strong, D. F., 1988, Geochemical studies of alkali feldspars in lithophile element-rich granitic suites from Newfoundland, Nova Scotia and Peru: Geological Association of Canada-Mineralogical Association of Canada Abstracts with Programs, v. 13, p. 68.

Korzhinskiy, M. A., 1981, Apatite solid solution as indicators of the fugacity of HCl and HF in hydrothermal fluids: Geochemistry International, v. 18, p. 44–60 (translated from Geokhimiya, 1981, v. 5, p. 689–706).

Latil, C., and Maury, R., 1977, Contribution à l'étude des échanges d'ions OH, Cl et F et de leur fixation dans les apatites hydrothermales: Bulletin de la Société Français de Minéralogie et de Cristallographie, v. 100, p. 246–250 (in French).

London, D., 1990, The berlinite substitution, AlP = 2Si, in alkali feldspars from differentiated peraluminous igneous rocks (granites, pegmatites, and rhyolites): Geological Society of America Abstracts with Programs, v. 22, p. 346.

London, D., Černý, P., Loomis, J. L., and Pan, J. J., 1990, Phosphorus in alkali feldspars of rare-element granitic pegmatites: Canadian Mineralogist, v. 28, p. 771–786.

London, D., Loomis, J. L., and Huang, W., 1990, Behavior and effects of phosphorus in the system Ab-Or-Qz-H2O at 200 MPa (H2O): Geological Society of America Abstracts with Programs, v. 22, p. 302.

Luhr, J. F., 1990, Experimental phase relations of water- and sulfur-saturated arc magmas and the 1982 eruptions of El Chichón Volcano: Journal of Petrology, v. 31, p. 1071–1114.

Mandel, J., 1964, The statistical analysis of experimental data: New York, Dover, 410 p.

Montel, J. M., Mouchel, R., and Pichavant, M., 1988, High apatite solubilities in peraluminous melts: Terra Cognita, v. 8, p. 71.

Munoz, J. L., 1990, F and Cl contents of hydrothermal biotites: A re-evaluation: Geological Society of America Abstracts with Programs, v. 22, p. 135.

Nekvasil, H., 1988a, Calculation of equilibrium crystallization paths of compositionally simple hydrous felsic melts: American Mineralogist, v. 73, p. 956–965.

———— 1988b, Calculated effect of anorthite component on the crystallization paths of H_2O undersaturated haplogranitic melts: American Mineralogist, v. 73, p. 966–981.

Parry, W. T., 1972, Chlorine in biotite from Basin and Range plutons: Economic Geology, v. 67, p. 972–975.

Parry, W. T., and Jacobs, D. C., 1975, Fluorine and biotite in Basin and Range Plutons: Economic Geology, v. 70, p. 554–558.

Perkins, D., Essene, E. J., and Wall, V. J., 1987, THERMO: A computer program for calculation of mixed-volatile equilibria: American Mineralogist, v. 72, p. 446–447.

Piccoli, P. M., *ms*, 1992, Apatite Chemistry in Felsic Magmatic Systems: Ph.D. thesis, University of Maryland at College Park, 293 p.

Piccoli, P. A., and Candela, P. A., 1988, Trends in apatite chemistry from El Chichón: Implications for vapor evolution: Geological Society of America Abstracts with Programs, v. 43, p. 1419.

———— 1991, Spatial variations in model halogen concentrations in magmas based on apatite chemistry: Examples from natural systems: Geological Society of America Abstracts with Programs, v. 23, p. 32.

———— 1992, Interpretation of the chemistry of the mineral apatite from granitic rocks: a preliminary model calculation for the estimation of initial halogen contents in the Tuolumne Intrusive Suite, Sierra Nevada Batholith, California, *in* Abstracts from the Second Hutton Symposium on the Origin of Granites and Related Rocks: Transactions of the Royal Society of Edinburgh, Earth Sciences, v. 83, p. 496.

Pichavant, M., Montel, J. M., and Richard, L. R., 1992, Apatite solubility in peraluminous liquids: Experimental data and an extension of the Harrison-Watson model: Geochimica et Cosmochimica Acta, v. 56, p. 3855–3861.

Piwinskii, A. J., 1968, Experimental studies of igneous rock series, central Sierra Nevada Batholith, California: Journal of Geology, v. 76, p. 548–570.

Piwinskii, A. J., and Wyllie, P. J., 1967, Experimental studies of igneous rock series: a zoned pluton in the Wallowa Batholith, Oregon: Journal of Geology, v. 76, p. 205–234.

———— 1970, Experimental studies of igneous rock series: Felsic body suite from the Needle Point Pluton, Wallowa Batholith, Oregon: Journal of Geology, v. 78, p. 52–76.

Potts, P. J., 1987, A Handbook of Silicate Rock Analysis: London, Blackie and Son Limited, 622 p.

Reid, J. B., Jr., Evans, O. C., and Fates, D. G., 1983, Magma mixing in granitic rocks of the central Sierra Nevada, California: Earth and Planetary Science Letters, v. 66, p. 243–261.

Robie, R. A., Hemingway, B. S., and Fisher, J. R., 1979, Thermodynamic properties of minerals and related substances at 298.15 K and 1 bar (10^5 Pascals) and at higher temperatures: United States Geological Survey Bulletin 1452, 456 p.

Roegge, S., Logsdon, M. J., Young, H. S., Barr, H. B., Borcsik, M., and Holland, H. D., 1974, Halogens in apatites from the Providencia Area, Mexico: Economic Geology, v. 69, p. 229–240.

Schmidt, M. W., 1992, Amphibole composition in tonalite as a function of pressure: an experimental calibration of the Al-in-hornblende barometer: Contributions to Mineralogy and Petrology, v. 110, p. 304–310.

Shinohara, H., *ms*, 1987, Partition of chlorine compounds in the system silicate melt and hydrothermal solutions: Unpublished D.Sc. Dissertation, Tokyo Institute of Technology, 192 p.

Shinohara, H., Iiyama, J. T., and Matsuo, S., 1984, Geochemistry-Behavior of chlorine in the system granitic magma-hydrothermal solution (in French): Académie Science Paris Comptes rendus, v. 298, Serie II, n° 17, p. 741–743.

———— 1989, Partition of Chlorine between silicate melt and hydrothermal solutions: I. Partition of NaCl-KCl: Geochimica et Cosmochimica Acta, v. 53, p. 2617–2630.

Sisson, V. B., 1987, Halogen chemistry as an indicator of metamorphic fluid interaction with the Ponder pluton, Coast Plutonic Complex, British Columbia, Canada: Contributions to Mineralogy and Petrology, v. 95, p. 123–131.

Skirius, C., and Anderson, A. T., Jr., 1988, Pre-eruptive H2O and CO2 across the plinian to ash-flow transition of the Bishop Tuff: EOS (Transactions of the American Geophysical Union), v. 69, p. 529.

Stollery, G., Borcsik, M., and Holland, H. D., 1971, Chlorine in intrusives: a possible prospecting tool: Economic Geology, v. 66, p. 361–367.

Stormer, J. C., Jr., Pierson, M. L., and Tacker, R. C., 1991, Anisotropic variation of F and Cl x-ray intensity in apatite due to diffusion during exposure to an electron beam: Geological Society of America Abstracts with Programs, v. 23, p. 220.

Stull, D. R., and Prophet, H., 1971, JANAF thermochemical tables: National Standard Reference Data Service, United States National Bureau of Standards, v. 37, 1141 p.

Sudarsanan, K., and Young, R.A., 1978, Structural interactions of F, Cl, and OH in apatites: Acta Crystallographica, v. B34, p. 1401–1407.

Tacker, R. C., 1988, Contrasting volatile behavior in the Bishop Tuff and Fish Canyon Tuffs—the applications of apatite solid solutions: Geological Society of America Abstracts with Programs, v. 20, p. 114.

Tacker, R. C., and Stormer, J. C., Jr., 1989, A thermodynamic model for apatite solid solutions, applicable to high-temperature geologic problems: American Mineralogist, v. 74, p. 877–888.

Thompson, J. B., Jr., 1982, Compositional space: an algebraic and geometric approach, *in* Ferry, J. M., editor, Characterization of Metamorphism through Mineral Equilibrium: Reviews in Mineralogy, v. 10, p. 1–31.

Urabe, T., 1985, Aluminous granite as a source of hydrothermal ore deposits: Economic Geology, v. 80, p. 148–157.

———— 1987, The effect of pressure on the partitioning ratios of lead and zinc between vapor and rhyolite melts: Economic Geology, v. 82, p. 285–294.

Volfinger, M., Robert, J.-L, Vielzeuf, D., and Neiva, A. M. R., 1985, Structural control on the chlorine content of OH-bearing silicates (micas and amphiboles): Geochimica et Cosmochimica Acta, v. 49, p. 37–48.

Watson, E. B., 1979, Apatite saturation in basic to intermediate magmas: Geophysical Research Letters, v. 6, p. 937–940.

———— 1980, Apatite and phosphorus in mantle source regions: an experimental study of apatite/melt equilibria at pressures to 25 kbar: Earth and Planetary Science Letters, v. 51, p. 322–335.

———— 1991, Diffusion of dissolved CO_2 and Cl in hydrous silicic to intermediate magmas: Geochimica et Cosmochimica Acta, v. 55, p. 1897–1902.

Watson, E. B., and Harrison, T. M., 1984, Accessory minerals and geochemical evolution of crustal magmatic systems: a summary and prospectus of experimental approaches: Physics of the Earth and Planetary Interiors, v. 35, p. 19–30.

Webster, J. D., 1990, Partitioning of F between H2O and CO2 fluids and topaz rhyolite melt: Implications for mineralizing magmatic-hydrothermal fluids in F-rich granitic systems: Contributions to Mineralogy and Petrology, v. 104, p. 424–438.

Webster, J. D., and Holloway, J. R., 1988, Experimental constraints on the partitioning of Cl between topaz rhyolite melt and H2O and H2O + CO2 fluids: New implications for granitic differentiation and ore deposition: Geochimica et Cosmochimica Acta, v. 52, p. 2091–2105.

———— 1990, Partitioning of F and Cl between magmatic hydrothermal fluids and highly evolved granitic magmas, *in* Stein, H. J., and Hannah, J. L., editors, Ore-bearing Granitic Systems: Petrogenesis and mineralizing processes: Geological Society of America Special Paper 246, p. 21–34.

Whitney, J. A., 1975, The effects of pressure, temperature, and X(H2O) on phase assemblage in four synthetic rock compositions: Journal of Geology, v. 83, p. 1–31.

———— 1988, The origin of granite: The role and source of water in the evolution of granitic magmas: Geological Society of America Bulletin, v. 100, p. 1886–1897.

Williams, T. J., Candela, P. A., and Piccoli, P. M., 1991, An experimental determination of the equilibrium constant for hydrogen-sodium exchange between a high-silica rhyolite and a chloride-bearing, two-phase aqueous mixture at 800°C and 1 kilobar: EOS (Transactions of the American Geophysical Union), v. 72, p. 308.

Yardley, B. W. D., 1985, Apatite composition and the fugacities of HF and HCl in metamorphic fluids: Mineralogical Magazine, v. 49, p. 77–79.

Zhu, C., and Sverjensky, D. A., 1991, Partitioning of F, Cl, and OH between minerals and hydrothermal fluids: Geochimica et Cosmochimica Acta, v. 55, p. 1837–1858.